Insights into the function of ataxin-3 via CRISPR gene knockout

Lorenza Villegas, 260774908

Integrated Program in Neuroscience

McGill University, Montreal

July 2020

A thesis submitted to McGill University in partial fulfillment of the requirements of the degree of Master of Science

Table of Contents

Abstract 4

Résumé 5

Acknowledgements 7

Contribution of Authors 9

List of Abbreviations 10

Introduction and Rationale 11

Background 12

Spinocerebellar Ataxia Type 3 12

Description of the disease 14

Genetics of SCA3 16

Ataxin-3 protein 17

Parkin: An E3 Ub-ligase 18

Ataxin-3 and Parkin interaction in the UPS 20

Mitochondrial dysfunction in SCA3 20

Project Objective and Aims 23

Methods 24

Generation of CRISPR knockout cell lines 24

HEK293T ataxin-3 KO cell line 24

U2OSn ataxin-3 KO cell line 25

Cell culture 26

Galactose-grown U2OSn ataxin-3 GFP-Parkin cell line 26

Transfection 27

U2OSn ataxin-3 GFP-parkin cell line 27

Antibody validation with immunofluorescence 27

Western blotting 27

Antibody Validation 27

Immunoblotting for parkin levels 28

Immunoblotting for parkin and mitochondrial protein levels 29
Immunofluorescence staining 30
Antibody validation 30
CCCP experiment for parkin recruitment 30
Importazole experiment for parkin recruitment 31
Antibodies 32
Live-cell fluorescent Imaging 33
CCCP experiment for parkin recruitment 33
Analysis of mitochondrial membrane potential 33
Cell cycle analysis 33
Determination of the rate of cell proliferation 34
Mitochondrial turnover assay 34
Statistical Analysis 35
Results 36
CRISPR knockout of ataxin-3 in cultured cells 36
Characterization and validation of ataxin-3 knockout lines 38
Antibody validation for WB 39
Antibody validation for IF 41
Measuring effects on cell proliferation and cell cycle timing 47
Observing the effect on parkin stability 51
Investigating parkin function in the mitophagy pathway 53
Generation of GFP-Parkin line using U2OSn ataxin-3 KO 53
Measuring mitochondrial membrane potential 54
Measuring parkin recruitment using CCCP 55
Measuring parkin recruitment in the presence importazole 60
Measuring parkin recruitment by WB 63
Measuring turnover in ataxin-3 KO cells 64
Discussion 65
Conclusion 79
References 82

Abstract

Spinocerebellar Ataxia Type 3 is a rare hereditary neurodegenerative disorder that is the most common form of ataxia in the world. This disease is characterized by a trinucleotide repeat expansion of CAG in the *ATXN3* gene, leading to an elongated polyglutamine tract in the ataxin-3 protein. In the disease, the abnormal form of ataxin-3 creates insoluble aggregates that ultimately accumulate in neurons, and whether this accumulation is neuroprotective or toxic, is still being elucidated. In normal conditions, endogenous ataxin-3 has been associated with several cellular pathways including ubiquitination, misfolded protein degradation, DNA damage, transcription, cytoskeletal organization and cell homeostasis, and has been implicated in the interaction with many proteins. Specifically, ataxin-3 interacts and binds with parkin, a protein involved in Parkinson's Disease. Parkin is an E3 ligase in the ubiquitin system and is also involved in mitochondrial quality control, as it removes oxidized cargo and damaged mitochondria from the cell. Ataxin-3 deubiquitinates parkin and impedes its ability to self-ubiquitinate. This project set out to investigate the effect of the absence of ataxin-3 removal on parkin function and stability in the cell as well as in the mitochondria quality control pathway, and the global effect of ataxin-3 absence in the cell. CRISPR-edited HEK293T and U2OSn ataxin-3 KO cell lines revealed successful deletion of *ATXN3* gene. Cell cycle analysis seemed normal in these KO lines, showing ataxin-3 removal might not impact cell cycle behavior. However, cell proliferation was reduced in HEK293T ataxin-3 KO cells, demonstrating a possible impact on cell growth. For parkin, immunoblotting and immunofluorescent experiments indicated ataxin-3 KO cells did not have changes in parkin levels, stability, and function. But there was a reduced impact on mitophagy in KO cells in mt-Keima experiment when quantifying mitochondrial turnover. This research revealed that ataxin-3 could have a potential role in mitochondrial quality control with parkin.

Résumé

L'ataxie spinocérébelleuse de type 3 est la forme la plus fréquente d'ataxie au monde. C'est une maladie neurodégénérative héréditaire rare, caractérisée par une expansion anormale du triplet de nucléotides CAG dans le gène *ATXN3*. Cette répétition se traduit par la présence d'une expansion polyglutaminique dans la protéine ataxine-3, entraînant la formation d'agrégats insolubles de la protéine anormale, qui s'accumulent dans les neurones. La nature neuroprotectrice ou toxique de ces agrégats reste à ce jour non déterminée. Dans sa forme normale, la protéine ataxine-3 interagit avec de nombreuses autres protéines, et est associée à différents mécanismes cellulaires telles que la voie d'ubiquitination, la dégradation des protéines mal repliées, l'altération de l'ADN, la transcription, l'organisation du cytosquelette, ou encore le maintien de l'homéostasie cellulaire. L'ataxine-3 interagit avec la protéine parkine, qui joue un rôle dans la maladie de Parkinson. La parkine est une enzyme de type ubiquitine ligase E3 impliquée dans le contrôle qualité des mitochondries, permettant la dégradation des protéines cargo oxydées et des mitochondries dysfonctionnelles.

L'ataxine-3 est responsable de la déubiquitination de la parkine et empêche son auto-ubiquitination. L'objectif de ce travail est d'étudier l'impact de l'absence de l'ataxine-3 sur la stabilité et la fonction de la parkine et sur le contrôle qualité des mitochondries, et plus généralement l'effet de son absence au niveau de la cellule. Lors de ce travail, des lignées de cellules HEK-293T et U2OSn ataxin-3 KO, déplétées de l'expression de l'ataxine-3 par la technique d'édition de génome CRISPR, ont été générées. Le cycle cellulaire de ces cellules est normal mais la prolifération des cellules HEK-293T ataxin-3 KO est diminuée, démontrant que la protéine ataxin-3 ne serait pas impliquée dans la régulation du cycle cellulaire, mais jouerait un rôle potentiel dans la prolifération des cellules. Des analyses par immunoblot et

immunocytochimie dans ces mêmes cellules ont mis en évidence que l'absence d'expression de l'ataxine-3 n'a pas d'effet sur le niveau d'expression, sur la stabilité, ou sur la fonction de la parkine. Enfin, l'analyse de la mitophagie dans des cellules ataxin-3 KO exprimant la protéine mito-Keima a montré une faible diminution de celle-ci. Cette recherche a ainsi mis en évidence le rôle potentiel de l'ataxine-3 dans le contrôle qualité des mitochondries, en association avec la parkine.

Acknowledgements

To my supervisor, Dr. Thomas Durcan, who gave me encouragement, support and permanent guidance to complete this investigation. Thank you for your input and patience from the beginning and for believing in me. Thank you allowing me to be part of your valuable team during these 3 years. Thank you for letting me undertake this project, which holds a special place for you, and evolving the story further. Your great heart, professionalism and dedication made me become a scientific professional and I am sure I will leave facing my future challenges with great responsibility. A true leader is not only that one who beacons guidance and gives light, but it's also the one that takes your hand and shows you that growth over time will bear fruits. That is what you are!

To my committee members: Dr. Edward Fon and Dr. Gary Armstrong. Thank you for your scientific brainstorming, excellent insights and questions, motivation to keep me pushing forward, and most importantly your patience. Your timely and accurate contributions made the discussions enriching in each of the stages carried out in this project. You are participants of my first steps as a scientist.

To my two laboratory godmothers, Genevieve and Lenore. Both of you were there for me as I succeeded and as I struggled. You helped me see the light in the darkness, picked me up when I was down, and cheered me on when I was motivated. Genevieve, you guided me to always make the correct decisions in my research and taught me more than you think. Lenore, you were always there by my side. I want to thank you in a very special way for your availability and generosity to share your extensive knowledge and experience with me. I thank you for your attentive and quick responses to the different concerns and corrections that arose during the development of my thesis. I will never forget you both.

To my laboratory team and fellow lab partners, endless gratitude goes out to every single one of you. It was inspiring for me to be in contact with such professional people dedicated to science with the constant desire to help humanity. Thank you for your input, for your questions, for sharing your knowledge with me during work hours; and for the laughs and the good times outside the lab. Thank you for making me feel part of a scientific family. Each one of you left a seed of knowledge, companionship and example. I hope that I can share my future successes with each one of you. I will carry you in my heart always remembering that we are a winning team, and that each one of you shines like a quasar in the universe and I will see you shine wherever I am in the world.

To my parents and family, for infinite support, advice and encouragement. For not having a clue what I'm studying but still taking the time to understand the academic lifestyle. Thank you for giving and wishing me the best always. To my parents who are my inspiration and constant love. Thank you, dad, for allowing me to fulfill my dreams, and to you, mom, for accompanying me during this journey. You are both an example of struggle, honesty and love. Thank you for being the best cheerleaders life can give me: I am nothing without you.

Thank you to McGill University and the Montreal Neurological Institute for allowing me to start this journey and for allowing me to live such an important experience for my training and work as a researcher. Thank you for having provided me with the necessary elements, materials and means to complete my thesis. Thank you to the IPN team for guiding me academically and for always being there to help with any question necessary.

To each and every person who joined and participated in this process: you were responsible for allowing me to complete this goal.

Contribution of Authors

The author generated the text, data, and figures in this thesis, except where indicated here.

Genevieve Dorval participated in the design of the CRISPR gRNAs.

Dr. Faiza Benaliouad created the U2OSn knock-in line that stably expresses Cas9.

Dr. Carl Laflamme generated the mosaic approach used for the immunofluorescent experiments and was published prior to this thesis.

Dr. Julien Sirois contributed to the analysis and generated the images of the cell cycle analysis in Figure 10. He also sorted the GFP-Parkin positive cells for the stable U2OS ataxin-3 KO GFP-Parkin cell line and generated the FACS reports on Figure 13.

Dr. Wolfgang Reintsch performed the cell proliferation analysis and generated the graphs for Figure 11.

Dr. Vincent Soubannier contributed to the analysis of mitochondrial membrane potential experiment in Figure 14, and the assay was performed by both the author and Dr. Soubannier.

Emma MacDougall contributed to the data analysis of parkin recruitment in Figure 16.

Dr. Lenore K. Beitel assisted in the editing of this thesis.

Dr. Mathilde Chaineau contributed to the French translation of the abstract.

Making of CRISPR KO, generation of stable cell lines, all protein and DNA extraction, cell culture, screening of antibodies, imaging and data analysis were performed by the author.

List of Abbreviations

- aa, amino acid
- ADCA I, autosomal dominant cerebellar ataxias type I
- BSA, bovine serum albumin
- CCCP, carbonyl cyanide *m*-chlorophenyl hydrazone
- CHIP, C-terminus of Hsc70-interacting protein
- Chk1, checkpoint kinase 1
- CNS, central nervous system
- CRISPR/Cas9, clustered regularly interspaced palindromic repeats
- CRM1, chromosomal maintenance 1
- COA7, cytochrome C oxidase assembly factor 7
- DMEM, dulbecco's modified eagle's medium
- DNA, deoxyribonucleic acid
- DRPLA, dentatorubral-pallidoluysian atrophy
- DUB, deubiquitinating enzyme
- eGFP, enhanced green fluorescent protein
- ERAD, endoplasmic-reticulum-associated protein degradation system
- ETC, electron transport chain
- FACS, Fluorescence-activated cell sorting
- GFP, green fluorescent protein
- gRNA, guide RNA
- HD, Huntington's disease
- HEK293T, human embryonic kidney cells
- HEPES, 4-(2-hydroxyethyl)-1-piperazineethanesulfonic acid
- HRP, horseradish peroxidase
- IBR, in-between-RING domain
- IF, immunofluorescence
- ITGA5, α5 integrin subunit
- KO, knockout
- MDV, mitochondrial-derived vesicle
- MEF, mouse embryonic fibroblast cells
- Mfn2, mitofusin 2 protein
- MJD, Machado-Joseph disease
- Mt-Keima, mitochondrially targeted keima protein
- NDUFA4, cytochrome C oxidase subunit
- NES, nuclear exporting signal
- NF-κB, nuclear factor kappa-light-chain-enhancer of activated B cells
- NLS, nuclear localization signal
- OMM, outer mitochondrial membrane
- PBS, phosphate-buffered saline
- PD, Parkinson's disease
- PI, propidium iodide
- PolyQ, polyglutamine
- pX459, pSpCas9(BB)-2A-Puro cloning vector
- RBR, RING-between-RING
- REP, repressor element of parkin
- RFP, red fluorescent protein
- RING, really interesting new gene
- RNF4, RING finger protein 4
- RIPA, radioimmunoprecipitation assay buffer
- SBMA, spinobulbar muscular atrophy
- SCA, spinocerebellar ataxia
- SCA3, spinocerebellar ataxia type 3
- SDHB, complex II succinate dehydrogenase ubiquinone iron–sulfur subunit
- SDS-PAGE, sodium dodecyl sulfate–polyacrylamide gel electrophoresis
- TMRM, tetramethylrhodamine, methyl ester
- TRD, trinucleotide repeat disorder
- U2OS, human bone osteosarcoma epithelial cells
- Ub, ubiquitin
- Ubl, ubiquitin-like
- UIMs, ubiquitin interacting motifs
- UPS, ubiquitin proteasomal system
- VCP/p97, valosin containing protein
- WB, western blot

Introduction and Rationale

Spinocerebellar Ataxia Type 3 (SCA3) is the most common dominantly inherited ataxia worldwide that is caused by excessive number of repeats of a CAG codon in the *ATXN3* gene, giving rise to an expansion in the polyglutamine tract of the ataxin-3 protein [1-3]. The mutant protein accumulates as insoluble aggregates within neurons of multiple brain regions involved in movement [4-7]. Ataxin-3 has been implicated in the ubiquitin system as a deubiquitinating enzyme, with potential roles in the misfolded protein degradation pathway of the Endoplasmic-Reticulum-Associated Protein Degradation (ERAD) system, as a transcriptional coactivator in oxidative stress response, and as an interactor with DNA repair proteins and histones in DNA repair [8-13]. As a deubiquitinating enzyme, ataxin-3 directly interacts with parkin, a Parkinson's Disease (PD) associated E3 ligase [14], by autoregulating its ubiquitinating activity and placing ubiquitin onto itself and not parkin. Expanded ataxin-3 increases clearance of parkin when it is recruited to the mitochondria and ultimately promotes parkin and mitochondrial degradation in cells, but the mechanism is yet to be discovered. Much of the research done on ataxin-3 has been carried out on with the mutated form, and gaps exist in how the wildtype protein functions, leaving similar unanswered questions, including how its partnership with parkin impacts on its overall function, and if together they might be important regulators in regulating mitochondrial quality control. Ever since gene editing techniques have become more advanced and readily available, we can now understand the role of a protein by knocking it out to see the effects of its absence. Thus, for this thesis, I used CRISPR genome editing to knockout the *ATXN3* gene and explore what happened in the absence of ataxin-3. In particular, examining the effects on the cell itself and mainly the impact on parkin stability and function, specifically with respect to the function of parkin at the mitochondria.

Background

Spinocerebellar Ataxia Type 3

Over forty years ago, a new genetic disorder was discovered. It was first documented in Azorean families as a hereditary disorder with common clinical and pathological characteristics[15]. Two recognized families with a heritable ataxia were descended from William Machado and Antone Joseph, thus the disorder was named Machado-Joseph Disease (MJD). In 1993, the genetic mutation was mapped to chromosome 14q32.1 by two different groups: the group studying the Azorean MDJ lineages [15], and another European group [16] that gave the name Spinocerebellar Ataxia Type 3 (SCA3) after realizing the similarity of symptoms to Spinocerebellar Ataxia Type 1 and Type 2 [15, 17-19]. This disease is characterized by an abnormal expansion of CAG trinucleotide repeats in the gene and in 1994, the cloning of the genetic loci demonstrated that the CAG expansion was the same for SCA3 and MJD, thereby uniting them into a single disorder. In this thesis, it will be referred as SCA3.

SCA3 is part of a subtype of trinucleotide repeat disorders (TRD). TRDs occur when a nucleotide repeat in the DNA has too many copies, causing a genetic mutation [20]. There are two classes of TRDs based on the mutations: non-coding triplet repeat diseases and coding triplet repeat diseases. In non-coding triplet diseases, the expansion lies in the non-coding region of the gene. Fragile X syndrome (CGG repeats) and Friedreich Ataxia (GAA repeats) are example of these diseases, where the trinucleotide expansion causes improper expression of the affected genes [21]. Coding triplet diseases have two subtypes, termed polyalanine diseases and polyglutamine (PolyQ) diseases. Polyalanine diseases have a unique feature where there is an imperfect repeat comprised of GC*N* repeats, where N describes any nucleotide. Oculopharyngeal

muscular dystrophy (GCG repeats) and synpolydactyly 1 disorder (GCN repeats) are examples of this class of disease [22, 23].

PolyQ diseases are the most common group of hereditary and neurodegenerative TRDs, and are characterized by the expansion of the CAG codon, which encodes glutamine, resulting in an expanded polyglutamine tract in the translated protein [24]. To date, ten CAG repeat disorders have been identified; which include the archetypal Huntington's disease (HD), spinobulbar muscular atrophy (SBMA), dentatorubral-pallidoluysian atrophy (DRPLA), and several types of spinocerebellar ataxias (SCA). There are currently 48 different types of SCAs [25, 26], but only seven of them have a trinucleotide repeat: SCA1, SCA2, SCA3, SCA6, SCA7, SCA12, and SCA17 [1, 3, 4, 24, 27-30]. The polyQ diseases are summarized on **Table 1**. For each disease, there is a critical threshold of polyQ expansion that has to be exceeded for disease onset to occur, and each mutated polyQ protein causes a separate and independent neurodegenerative disease that targets different populations of neurons [24]. The mechanisms by which the polyQ-expanded proteins lead to pathology in these diseases is not totally understood. There are, however, some similarities between the polyQ diseases. For instance, all mainly affect the central nervous system (CNS) and the peripheries/muscles are variably affected; the onset of symptoms is usually in adulthood, during the 3rd through 5th decade, and progress slowly over several years; most are autosomal dominant disorders, except SBMA which is inherited in an X-linked manner; protein aggregates accumulate and neuropathology occurs; and all are predictably fatal with no cure and no approved treatments to stop the disease evolution [3, 4, 24].

Disease	Common Name	Protein	Localization	Normal CAG	PolyQ CAG range
Huntington Disease		Huntingtin	Cytoplasm	6 - 35	36 - 121
Spinobulbar Muscular Atrophy	Kennedy's Disease	Androgen Receptor	Nucleus, Cytoplasm	6 - 36	38 - 65
Dentatorubral-pallidoluysian atrophy	Haw River Syndrome	Atrophin-1	Nucleus, Cytoplasm	3 - 38	49 - 88
Spinocerebellar Ataxia Type 1		Ataxin-1	Nucleus	6 - 39	39 - 88
Spinocerebellar Ataxia Type 2		Ataxin-2	Cytoplasm	14 - 32	33 - 77
Spinocerebellar Ataxia Type 3	Machado Joseph Disease	Ataxin-3	Nucleus, Cytoplasm	12 - 44	56 - 87
Spinocerebellar Ataxia Type 6		CACNA1A	Plasma Membrane	4 - 18	21 - 33
Spinocerebellar Ataxia Type 7		Ataxin-7	Nucleus, Cytoplasm	7 - 18	38 - 200
Spinocerebellar Ataxia Type 12		PPP2R2B	Cytoplasm	4 - 31	43 - 78
Spinocerebellar Ataxia Type 17		TATA-box Binding Protein	Nucleus	25 - 43	47 - 63

Table 1. PolyQ Diseases.

All CAG-repeat disorders with their corresponding protein, the localization of the affected protein, the normal CAG repeat, and the typical pathogenic polyQ range associated with each disease.

Description of the disease

SCA3 is a rare, hereditary, and progressive neurodegenerative disease. However, although rare, it is the most common dominantly inherited form of ataxia in the world, affecting on average 2.7 people in 100,000, and is second after HD in prevalence [3, 25, 31]. The disease has a worldwide distribution and high frequency in multiple countries, as represented by the percentage of individuals with SCA3 among the people suffering from dominant ataxias. These countries include China (62%), Brazil (59.6%), Portugal (58%) Taiwan (47.3%), Japan (43%),

Germany (42%), Canada (23.8%), United States (20%), Spain (15%), Australia (12%), Mexico (12%), India (7%), and Italy (1%) [32-36].

Neurodegeneration in SCA3 affects multiple regions within the brain, where the most significant feature of its neuropathology is the manifestation and accumulation of intraneuronal aggregates. Fundamentally, the brain regions affected include: the cerebellar hemispheres and the dentate nucleus in the cerebellum; the pons and the medulla oblongata in the brainstem; the thalamus and the substantia nigra in the midbrain; some cranial nerves; the occipital cortex; and the anterior horn and dorsal root ganglia in the spinal cord are affected, making this a multisystemic disorder [4-6, 28, 37]. These brain areas are principally involved in motor planning, motor execution, balance, and eye movement, which explains why individuals with SCA3 present a variety of progressive motor deficiencies over time. Whether these aggregates cause neuronal loss [38] or are neuroprotective [39] are still up for debate in the field.

There are various clinical characteristics in SCA3 patients, which gave rise to four subtypes of the disease, depending on their phenotypic presentation [40, 41]. The primary clinical hallmark of SCA3 is progressive cerebellar ataxia, which is a dysfunction of motor control and coordination that causes abnormal walking, speech, compromised balance, steady gaze and oculomotor abnormalities [1, 2, 4, 27, 28, 42, 43]. SCA3 also manifests with spasticity and hyperreflexia, parkinsonism with and without tremor, restless leg syndrome, nystagmus (uncontrolled repetitive eye movement), dystonia (uncontrolled muscle contractions), dysarthria (slurred speech), dysphagia (difficulty swallowing), and ophthalmoplegia (eye muscle paralysis/weakness) [3, 4, 30, 44]. Because of these neurological signs, SCA3 additionally belongs to the group of autosomal dominant cerebellar ataxias type I (ADCA I), a genetic subtype of

hereditary ataxia, characterized by these ataxic manifestations for SCA3, other SCAs and most ataxia disorders [26, 29, 45].

Nonmotor symptoms are less severe, but common, and include cognitive impairment, REM sleep disorder, olfactory dysfunction, stomach problems, and psychological/psychiatric conflicts [4, 43, 46, 47]. The neuronal loss of the substantia nigra and dentate nucleus of the midbrain and cerebellum account for the parkinsonian and ataxic phenotype, according to some researchers [42, 44]. Overall, failure in functions of the brainstem, mainly involved in dysphagia, is what usually leads to the death of patients within 10-15 years of symptom onset [48]. At present, there is no cure for SCA3; though treatments do exist to manage the motor symptoms of the disease.

Genetics of SCA3

The genetic defect responsible for this disease is an expansion of the CAG trinucleotide in the *ATXN3* gene resulting in an expanded polyglutamine tract in the ataxin-3 protein [2, 49, 50]. The expanded CAG length dwells in exon 10 of the *ATXN3* gene. In healthy individuals, the normal range of CAG repeats is between 12 to 44, with more than 90% of the population having fewer than 31 repeats; whereas in individuals with the expanded polyQ repeat it ranges from 56 to 87 CAGs. Those with CAG repeats between 45 to 55 are considered to be in the "gray zone," where they have an incomplete penetrance of symptoms [1, 4, 29, 43, 51]. Similar to the other PolyQ disorders, the length of the CAG expansion is inversely correlated with age of disease onset and directly correlates with disease severity, meaning that a greater number of such repeats result in an earlier and more severe development of the disease [1, 29]. Although rare, there have been homozygous SCA3 patients reported, where the individual receives two copies of the mutated *ATXN3* gene, which leads to much earlier onset and worsening of symptoms [52]. There are

currently no individuals who have been reported for haploinsufficiency, or are null, for the *ATXN3* gene [3].

Ataxin-3 protein

Ataxin-3 is a 42 kDa evolutionary conserved protein that is ubiquitously expressed in the body with strong expression in the CNS and is localized throughout the cell. It can move in and out of the nucleus, and although in the majority of studies it appears to be generally nuclear and cytoplasmic in cells, and it has also been observed in axons and in mitochondria [7, 50, 53]. It has a nuclear localization signal (NLS) between aa 282-285 and two nuclear export signals (NES) aa 77-99 and aa 141-158 [54]. Ataxin-3 is an incompletely characterized protein, and its exact biological function(s) are still being explored. However, the protein has been implicated in a broad range of cellular processes including deubiquitination, misfolded protein degradation in the ERAD system, autophagy, transcriptional regulation, DNA repair, cytoskeletal organization, and cell quality control [2, 40]. Ataxin-3 possesses several domains that contribute to its function (**Figure 1**).

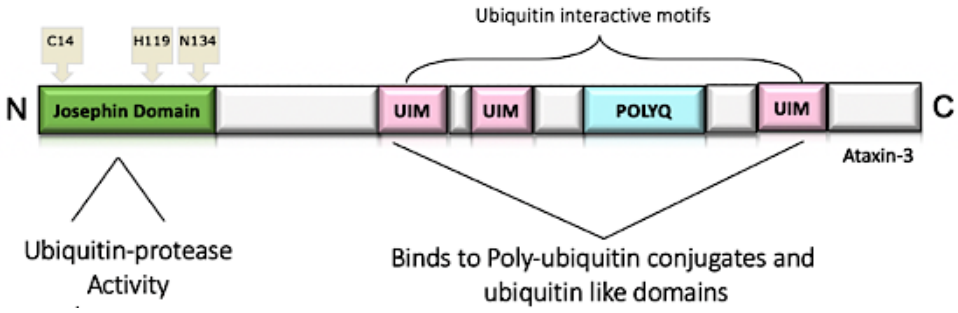

Figure 1. Schematic of the ataxin-3 protein.
Within its N-terminal is the Josephin Domain, a domain where a cysteine protease fold resides. Its C-terminal tail consists of three UIMs that binds to Ub conjugates, and the polymorphic polyQ region in between UIM 2 and 3.

The structured globular N-terminus contains the highly conserved Josephin Domain responsible for catalytic cleavage of ubiquitin (Ub) chains. Ub is a small protein ubiquitously expressed in all eukaryotic cells with a well-known role in targeting proteins for degradation as well as several other functions [55]. The flexible C-terminal tail contains three Ub interacting motifs (UIMs) and an unstructured polymorphic polyQ tract. Through its UIMs, ataxin-3 can bind to Ub conjugates and also Ub-like (Ubl) containing proteins [3, 56]. Full length 3UIM ataxin-3 is the major isoform expressed in the brain, no matter the age and size of the polyQ expansion [57]. In contrast, the originally cloned 2UIM isoform, although enzymatically identical, is highly unstable, aggregate-prone and not detected in brain tissue.

Mounting evidence has suggested that ataxin-3 is involved in the Ub proteasomal system (UPS), one of the major pathways for turnover and degradation of proteins. As a deubiquitinating enzyme (DUB) in the UPS, ataxin-3 is able to bind through its UIMs to K48-linked Ub conjugates that signal for proteasomal degradation and K63-linked chains that are involved in autophagy/signaling/DNA repair [37, 58]. It functions in a unique way by shortening polyUb chains rather than completely disassembling them, thereby inhibiting protein degradation of its interacting partners [9, 59]. Ataxin-3 has been shown to interact with multiple E3 Ub ligases, a class of proteins involved in assembling Ub conjugates on other proteins substrates and on themselves, such as C-terminus of Hsc70-interacting protein (CHIP); Gp78, an ER associated E3; and SUMO-specific RING Finger Protein 4 (RNF4) [59-61].

Parkin: An E3 Ub-ligase

Importantly, ataxin-3 was the first DUB identified to partner with the E3 Ub ligase parkin [8]. Parkin is a RING-Between RING (RBR) type E3 Ub ligase of the UPS, and mutations in parkin account for 50% of adolescent juvenile patients diagnosed with PD [14, 62]. As an E3,

parkin determines how Ub chains are assembled on substrate proteins, as well as regulating its own activity via self-ubiquitination. Specifically, at the N-terminus, parkin contains a Ubl domain that is involved in substrate and proteasomal recognition, regulating cellular activity, and binding to Ub-binding domains, such as UIM containing proteins. At the C-terminus, parkin has three RING motifs (RING0, RING1, RING2), with the RING2 possessing an active site cysteine through which parkin can form a parkin-Ub thioester complex, from which it can transfer the Ub onto one of its substrates. Additional domains include the repressor element of parkin (REP) domain that regulates its activity, and an in-between-RING (IBR) domain between RING1 and RING2, hence parkin being a RBR-type E3 ligase [8, 63, 64] (**Figure 2**).

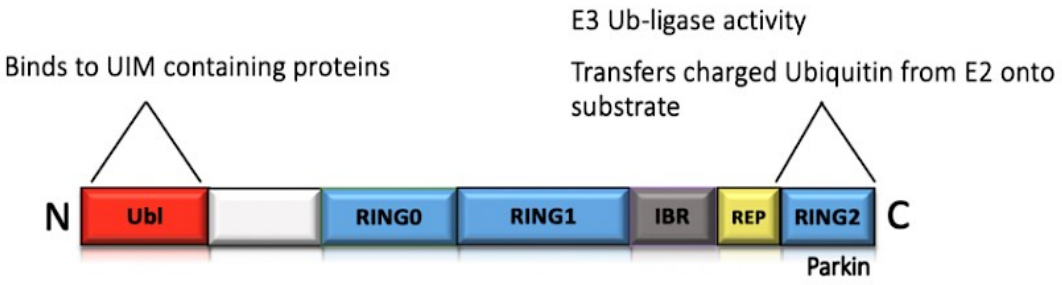

Figure 2. Schematic of the parkin protein.
The N-terminus of parkin contains a Ub-like domain, allowing it to interact with Ub-binding domains. It also has three RING motifs (RING0, RING1, RING2). The RING2 domain possesses its E3 ligase activity, a Repressor Element of Parkin (REP) domain regulates its activity, and an in-between-RING (IBR) domain between RING1 and RING2 at the C-terminus.

Parkin is a cytoplasmic protein that is centrally involved in mitochondrial quality control, as parkin can mediate the removal of mitochondrial vesicles containing oxidized cargo, or in some cases the entire mitochondria though a process called mitophagy [63, 65-67]. In mitophagy, parkin is recruited onto dysfunctional mitochondria, ubiquitinates outer membrane proteins, and ultimately targets mitochondria for autophagic degradation [8, 65, 68].

Ataxin-3 and Parkin interaction in the UPS

Ataxin-3 binds the Ubl of parkin through its UIMs, regulating the auto-ubiquitination activity of parkin by deubiquitinating parkin through a process that redirects the Ub away from Parkin and onto itself, through a process that requires the active cysteine in the Josephin Domain of ataxin-3 (**Figure 3**).

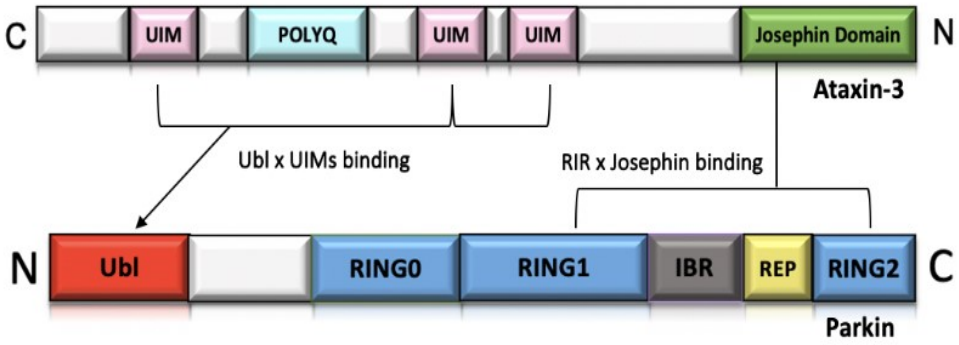

Figure 3. Binding interaction between ataxin-3 and parkin.
The C-terminal UIMs of ataxin-3 bind to the N-terminal Ubl domain of parkin, and the conserved Josephin Domain binds to the RINGs of parkin.

This has been confirmed *in vitro* using HEK293 cells, where wildtype and expanded ataxin-3 reduced self-ubiquitination of parkin [8], and the same research further confirmed with a catalytically inactive ataxin-3 that it was not able to deubiquitinate parkin, thus showing that ataxin-3 actively deubiquitinates parkin through a unique mechanism distinct from other DUBs, as it fails to cleave Ub conjugates on parkin.

Mitochondrial dysfunction in SCA3

There is increasing evidence that shows ataxin-3 might influence mitochondrial dynamics [50, 68-73]. In SCA3, cleaved fragments of expanded ataxin-3 were shown to elevate toxicity and

nuclear aggregates. These toxic fragments increase mitochondrial fission in patient-derived cell lines, transgenic mice models and mouse embryonic fibroblasts (MEFs) causing dysregulation and eventually cell death which finally lead to neurodegeneration [68, 69, 74]. Expanded ataxin-3 associates with mitochondria and interacts with mitochondrial proteins *in vivo*. The cytochrome C oxidase subunit NDUFA4 (NDUFA4), the complex II succinate dehydrogenase (ubiquinone) iron–sulfur subunit (SDHB), and cytochrome C oxidase assembly factor 7 (COA7) were found to be enriched with expanded ataxin-3 compared to wildtype by mass spectrometry, which suggests stronger interactions [75]. Additionally, mitochondria from SCA3 mice had compromised complex II activity, and the same researchers also observed this decreased activity in PC6-3 neuronal-like cells with expanded polyQ ataxin-3 [76]. Regarding ataxin-3's localization, while ataxin-3 is mostly present in cytosolic fraction, it was also shown to be present in the mitochondrial fractions of HEK293T cells [50, 75].

This information is consistent with previous findings where reduced mitochondrial membrane potential, increased oxidative stress and mitochondrial DNA damage were found in SCA3 patients and mouse models [69-73]. It is known that ataxin-3 interacts and deubiquitinates parkin, but intriguingly the expanded form of ataxin-3 degrades parkin with greater efficiency than wildtype ataxin-3 [8]. It is predicted that expanded polyQ fragments of ataxin-3 interact with and damage the mitochondria, and could potentially recruit parkin and ultimately triggering mitophagy of the parkin-bound mitochondria altogether; ultimately reducing the levels of parkin in cells through prolonged autophagy [77]. All these studies highlight that dysregulation of mitochondrial function and the altered interaction between expanded ataxin-3 and the mitochondria is a contributing factor in the pathogenesis of SCA3.

Mitochondrial dysfunction is commonly involved in neurodegenerative diseases like PD, HD and SCA3 [68, 75, 77]. Interestingly, a marked feature of patients with SCA3 is the presentation of symptoms resembling those of PD patients. These parkinsonian features and clinical overlap have helped point to a protein-protein interaction of ataxin-3 and parkin, since they bind to each other and simultaneously play opposing roles in the UPS, which may account for the potential crosslink between both diseases.

Project Objective and Aims

The objective of this research was to create knockout cell lines of ataxin-3 and determine the long-term consequence of its absence on parkin stability and function, with a particular focus on the mitochondrial quality control pathway.

Delineating the function of ataxin-3 is critical as we work to explore the molecular underpinnings of SCA3 and understand how the interaction between parkin and ataxin-3 affects cellular processes, and in particular the well-documented function of parkin in mitochondrial quality control. Moreover, this work will help deepen our understanding of previous findings, as well as to determine whether a loss in functional ataxin-3 impacts pathways that may also be affected in SCA3 when levels of the wildtype protein are reduced.

The specific aims of the research project were the following:

1. Generate an ataxin-3 knockout model using CRISPR genome editing in distinct cell lines
2. Characterize and validate ataxin-3 knockout lines and test for effects on cell proliferation and cell cycle timing
3. Determine the effects on parkin levels in the absence of ataxin-3
4. Elucidate whether ataxin-3 deficiency impacts the function of parkin in the mitochondrial quality control pathway

Methods

Generation of CRISPR knockout cell lines

Two pairs of gRNAs were designed (sequences 5'TGCCTGAATAACTTATTGCA and 5'AGGATGAGAATGGCAGAAGG), specifically targeting exon 2 of *ATXN3* gene (ENSG00000066427) using the online tool CRISPR Direct http://crispr.dbcls.jp.
PCR screening primers are forward: CAAGAAGGCTCACTTTGTGCTC
and reverse: CAGGTAGTTGAAGCAAGGGTG.

Human embryonic kidney (HEK) 293T cells (ATCC® CRL-3216™) and human bone osteosarcoma epithelial cells (U2OS) cells (ATCC® HTB-96™) were used for the generation of KO cell lines. Both cell types are highly transfectable and in the top five cell lines for endogenous levels of the ataxin-3 protein (https://pax-db.org/protein/1858089).

HEK293T ataxin-3 KO cell line

The CRISPR KO was first started in HEK293T cells using the pSpCas9(BB)-2A-Puro (pX459) cloning vector (Addgene plasmid #48139) as the backbone [78]. To determine genome targeting efficiency for each gRNA, a T7 Endonuclease I assay (New England BioLabs® cat# M0302) was performed and two gRNAs were identified that effectively cleaved the *ATXN3* gene. The gRNAs in the vector were transfected using the JetPRIME® transfection protocol (from Polyplus) within a 6-well plate of 70% confluent cells, where the cells were seeded 24h prior to transfection. For transfecting the cells, 2µg of vector DNA was added into 200µl of JetPRIME buffer, followed by the addition of 4µl of JetPRIME reagent, before a 10-minute incubation at room temperature. Into each well, 200µl of transfection mix was added and distributed evenly onto the cells in 2ml of Dulbecco's modified Eagle's medium (DMEM).

Two days post-transfection, the polyclonal population was selected with 2µg/ml of puromycin and subsequently the cells were separated using fluorescence-activated cell sorting (FACS). Using the FACSAria™ Fusion Flow Cytometer from BD Biosciences (Cat# 6567OOG5), individual cells were isolated before being grown and expanded into individual cell colonies for screening. Twenty sorted cells produced a single clonal colony and after 2 weeks these clones were subsequently expanded and split into separate plates, with one plate frozen down as a backup and the other plate retained for PCR genotyping to identify clones in which the gene was successfully knocked out. Genomic DNA of clones were harvested using QuickExtract DNA extraction solution (Epicentre Biotechnologies) for DNA amplification by PCR, to confirm whether the *ATXN3* sequence was disrupted and a KO had occurred.

U2OSn ataxin-3 KO cell line

Using the same gRNA sequence as the HEK293T cells, synthetic gRNAs from Synthego were created. In U2OS cell lines, the Cas9 protein is not expressed, so a knock-in line was created in our lab using nucleofection and FACS selection that stably expressed Cas9 under the expression of a doxycycline (dox)-inducible promoter based on the manuscript from Mandegar et al [79]. With this method, one can quickly and efficiently produce loss-of-function phenotypes in iPSCs and other cell-type derivatives to study disease and developmental mechanisms. Introducing a single dox-inducible vector system into the AAVS1 safe harbor locus enables tight transcriptional control of Cas9 for gene KO studies upon the addition of dox. This TetO inducible vector system helps control the precise timing of knocking out the expression of target genes in a clonal cell carrying the designed gRNA of interest [79]. Once expressed, Cas9 complexes with gRNA, and cuts the gene in the targeted region. We refer to this dox-inducible cell line as U2OSn. These cells were plated with 2µg/mL of dox 48h before transfection. The

synthetic gRNAs were then transfected using the HiPerFect® transfection protocol from QIAGEN, dox was re-added the next day after transfection, and cells were cultured for an additional 48h. Next, the mixed population of cells were sorted, and clones were screened as outlined for the HEK293T ataxin-3 KO clones.

Cell culture

All cell lines were cultured at 37°C in a humidified atmosphere with 5% CO_2 in DMEM supplemented with 10% tetracycline-free FBS, 1% L-glutamine, 100 U/mL penicillin-streptomycin; except for the cells cultured with galactose media.

Galactose-grown U2OSn ataxin-3 GFP-Parkin cell line

DMEM 1X without glucose, sodium pyruvate, or glutamine was used to create the galactose media. 10mM galactose, 10mM HEPES, 1mM sodium pyruvate, 4mM glutamine, and 10% tetracycline-free FBS was added to this media to make galactose-containing DMEM. U2OSn ataxin-3 KO GFP-Parkin cells were passaged and plated in individual 15cm dishes for each KO and parental cell line and kept in galactose media for 2 weeks. After the cells were acclimated to galactose-containing media, galactose U2OSn ataxin-3 KO GFP-parkin cell lines were used for experiments. In parallel, U2OSn ataxin-3 KO (+/- GFP-Parkin) cells were cultured in glucose media.

Transfection

U2OSn ataxin-3 GFP-parkin cell line

U2OSn ataxin-3 KO cells and wildtype were transfected with a pEGFP-Parkin WT plasmid (Addgene plasmid #45875) [64] using JetPRIME® transfection, and then selected using 500µg/mL of G418 (Geneticin) (InvivoGen) for 10 days in order to create a stable cell line. After selection, the cells were sorted for GFP-positive cells the using FACSAria™ Fusion Flow Cytometer, expanded, kept in culture, or frozen down for backups.

Antibody validation with immunofluorescence

For the mosaic approach, 200,000 parental cell line cells were transiently transfected in one well of a 6-well plate with 1µg of the LAMP1 green fluorescent protein vector (GFP) (Addgene #16290) and the ataxin-3 KO cell line with 1µg of the LAMP1 red fluorescent protein vector (RFP) (Addgene #1817) using the JetPRIME® transfection protocol. At 24h post transfection, both cell lines were plated on glass coverslips in a 24-well plate as a mosaic and incubated for 24h.

Western blotting

Antibody Validation

Five HEK293T and four U2OSn ataxin-3 KO clones plus their respective parental cell lines were lysed in RIPA lysis buffer (20mM Tris-HCL, pH 7.4, 150mM NaCL, 1% Nonidet P-40) and cOmplete™ protease inhibitor cocktail (Sigma #11836153001). Protein concentrations were determined with the Bradford protein assay (BioRad, Hercules, California, USA), and 30µg

of protein extract was loaded in a 10% SDS-PAGE gel. The proteins were transferred onto nitro cellulose membranes (BioRad) by Bio-Rad Gel transfer system. Membranes were then blocked with 5% milk in TBS-Tween 0.01% for 1h and incubated with anti-ataxin-3 Millipore MAB5360 mouse monoclonal 1H9, Thermo Fisher MA3-082 mouse monoclonal, ProteinTech #13505-1-AP rabbit polyclonal, ElabScience E-AB-60279 rabbit polyclonal, and Abcam ab96316 rabbit polyclonal overnight at 4°C. All antibodies were used in 1:1000 dilution. Membranes were washed three times with TBS-Tween 0.01% the next day and incubated with secondary horseradish peroxidase (HRP) conjugated antibody for 1h at room temperature. Clarity substrate from BioRad was used for HRP detection of the antibodies, and chemiluminescent signals were then detected with BioRad ChemiDoc Touch imaging system.

Immunoblotting for parkin levels

To look at baseline levels of parkin in ataxin-3-depleted cells, 250,000 HEK293T ataxin-3 KO cells were seeded on a 6-well plate. Cells were lysed in RIPA lysis buffer (20mM Tris-HCL, pH 7.4, 150mM NaCL, 1% Nonidet P-40) and cOmplete™ protease inhibitor cocktail (Sigma #11836153001). Protein concentrations were determined with the Bradford protein assay (BioRad, Hercules, California, USA), and 30µg of protein extract was loaded in a 10% SDS-PAGE gel. The proteins were transferred onto nitro cellulose membranes (BioRad) by Bio-Rad Gel transfer system. Membranes were then blocked with 5% milk in TBS-Tween 0.01% for 1h and incubated with Thermo Fisher Parkin Monoclonal antibody #702785 (1:1000), validated MAB5360 Ataxin-3 antibody (1:1000), and ab2787 HSP70 (1:1000) as a loading control overnight at 4°C. Membranes were washed three times with TBS-Tween 0.01% the next day and incubated with secondary horseradish peroxidase (HRP) conjugated antibody for 1h at room

temperature. Clarity substrate from BioRad was used for HRP detection of the antibodies, and chemiluminescent signals were then detected with BioRad ChemiDoc Touch imaging system.

For the LI-COR immunoblotting, HEK293T ataxin-3 KO cells were lysed in RIPA lysis buffer (20mM Tris-HCL, pH 7.4, 150mM NaCL, 1% Nonidet P-40) and cOmplete™ protease inhibitor cocktail (Sigma #11836153001). Protein concentrations were determined with the Bradford protein assay (BioRad, Hercules, California, USA), and 100µg of protein was loaded on a 10% SDS-PAGE gel. The proteins were transferred onto nitro a cellulose membrane (BioRad) by Bio-Rad Gel transfer system. For quantitative immunoblot, the membrane was incubated with REVERT total protein stain to quantify the amount of protein per lane, and then blocked in Odyssey Blocking buffer (TBS) and incubated with Thermo Fisher Parkin Monoclonal antibody #702785 (1:1000) and validated MAB5360 Ataxin-3 antibody (1:1000) on the same membrane overnight at 4°C. The secondary antibodies (Odyssey IRDye 800CW and 700CW) were incubated in a 1:20000 dilution in TBST with 5% BSA for 1h at room temperature followed by three washes. Detection of the immunoreactive bands of both protein levels were performed by image scan using LI-COR Odyssey 9120 Imaging System (LI-COR Biosciences).

Immunoblotting for parkin and mitochondrial protein levels

In 200,000 U2OSn ataxin-3 KO GFP-Parkin cells in a 6-well plate, 20µM of carbonyl cyanide *m*-chlorophenyl hydrazone (CCCP) was added for 0h, 2h, 4h, and 24h. The cells were lysed, and the results were observed via immunoblotting 30µg of protein on a 10% SDS-PAGE gel. Membranes were blotted with Thermo Fisher Parkin Monoclonal antibody #702785 (1:1000), validated MAB5360 Ataxin-3 antibody (1:1000), outer mitochondrial membrane

protein Sigma-Aldrich CB1020 Mitofusin2 (1:1000), and MAB1501 Actin (1:5000) as loading control.

Immunofluorescence staining

Antibody validation

U2OSn ataxin-3 KO cells were cells were plated on 24-well plates with coverslips and fixed with room temperature 4% paraformaldehyde for 20 minutes at room temperature, permeabilized with 0.2% Triton X-100/PBS for 10 minutes and blocked in 0.05% Triton X-100/5% BSA/PBS for 1h. Coverslips were taken out from the plate and placed in a wet chamber and incubated with anti-ataxin-3 Millipore MAB5360 mouse monoclonal 1H9, Thermo Fisher MA3-082 mouse monoclonal, ProteinTech #13505-1-AP rabbit polyclonal, ElabScience E-AB-60279 rabbit polyclonal, and Abcam ab96316 rabbit polyclonal overnight at 4°C. All antibodies were used in 1:1000 dilution. The coverslips were incubated with secondary antibody in 0.05% Triton X-100/5% BSA/PBS for 1h at room temperature the following day and once washed, were mounted on glass slides ready for imaging. All five antibodies were screened using the mosaic strategy. Imaging was performed under the LEICA SP8 Confocal microscope using 40x oil objective and eGFP 488 Texas Red 570 and Alexa 638 HyD laser channels with pinhole aperture set to medium and Z focus set to 1µm per turn.

CCCP experiment for parkin recruitment

U2OSn ataxin-3 KO GFP-Parkin cells were treated with 20µM CCCP (Sigma cat# C2759) for 0h, 2h, 4h, and 6h in culture and after each hour cells were then fixed with room temperature 4% paraformaldehyde for 20 minutes at room temperature, permeabilized with 0.2%

Triton X-100/PBS for 10 minutes and blocked in 0.05% Triton X-100/5% BSA/PBS for 1h. Coverslips were taken out from the plate and placed in a wet chamber and incubated with the primary antibodies overnight at 4°C using validated ProteinTech #13505-1-AP ataxin-3 antibody (1:4000) and SantaCruz 17764 TOM20 antibody (1:1000) in 0.05% Triton X-100/5% BSA/PBS at 4°C. The coverslips were incubated with secondary antibody in 0.05% Triton X-100/5% BSA/PBS for 1h at room temperature the following day and once washed, were mounted on glass slides and observed in the LEICA SP8 Confocal microscope using 40x oil objective and eGFP 488, Texas Red 570 and Alexa 638 HyD laser channels with pinhole aperture set to medium and Z focus set to 1µm per turn.

Importazole experiment for parkin recruitment

To assay the rate of parkin recruitment in the presence of importazole, U2OSn ataxin-3 KO GFP-Parkin cells were treated with 40µM importazole (Sigma 401105) for 0h, 2h, 4h, and 6h in culture, then fixed with room temperature 4% paraformaldehyde for 20 minutes at room temperature, permeabilized with 0.2% Triton X-100/PBS for 10 minutes and blocked in 0.05% Triton X-100/5% BSA/PBS for 1h. Coverslips were taken out from the plate and placed in a wet chamber and incubated with the primary antibodies overnight at 4°C using validated ProteinTech #13505-1-AP ataxin-3 antibody (1:4000) and SantaCruz 17764 TOM20 antibody (1:1000) in 0.05% Triton X-100/5% BSA/PBS at 4°C. The coverslips were incubated with secondary antibody in 0.05% Triton X-100/5% BSA/PBS for 1h at room temperature the following day and once washed, were mounted on glass slides. Images were acquired using the LEICA SP8 confocal imaging system with a 40x oil objective and eGFP 488, Texas Red 570 and Alexa 638 HyD laser channels with pinhole aperture set to medium and Z focus set to 1µm per turn.

Antibodies

The following antibodies were used for immunoblotting:

Anti-Ataxin-3 (Millipore, cat# MAB5360) dilution 1:1000

Anti-Ataxin-3 (Thermo Fisher, cat# MA3-082) dilution 1:1000

Anti-Ataxin-3 (ProteinTech, cat# 13505-1-AP) dilution 1:1000

Anti-Ataxin-3 (ElabScience, cat# E-AB-60279) dilution 1:1000

Anti-Ataxin-3 (Abcam, cat# ab96316) dilution 1:1000

Anti-Parkin (Thermo Fisher, cat# 702785) dilution 1:1000

Anti-Mitofusin2 (Sigma-Aldrich, cat# CB1020) dilution 1:1000

Anti-HSP70 (Abcam, cat# ab2787) dilution 1:1000

Anti-Actin (Millipore, cat# MAB1501) dilution 1:5000

The following antibodies were used for immunofluorescence staining:

Anti-Ataxin-3 (Millipore, cat# MAB5360) dilution 1:1000

Anti-Ataxin-3 (Thermo Fisher, cat# MA3-082) dilution 1:1000

Anti-Ataxin-3 (ProteinTech, cat# 13505-1-AP) dilution

1:200, 1:1000, 1:2000, 1:4000, 1:5000, 1:10,000, 1:20,000

Anti-Ataxin-3 (ElabScience, cat# E-AB-60279) dilution 1:1000

Anti-Ataxin-3 (Abcam, cat# ab96316) dilution 1:1000

Anti-TOM20 (SantaCruz, cat# 17764) dilution 1:1000

* Note: After careful review, it was discovered both Millipore MAB5360 and Thermo Fisher MA3-082 are the same clone of an anti-ataxin-3 antibody. The duplicate clone was kept to determine if the binding was consistent between experimental applications, which indeed was the case.

Live-cell fluorescent Imaging

CCCP experiment for parkin recruitment

Galactose and glucose-grown U2OSn ataxin-3 KO GFP-Parkin cells were seeded in a four-chamber dish (Greiner cat# 627870) with 70,000 cells 24h before the start of acquisition. The next day the cells were first treated with 50nM MitoTracker deep red (ThermoFisher cat# M22426) for 15 minutes, washed with corresponding DMEM and incubated for 10 additional minutes. Cells were then washed twice with PBS and then FluoroBrite DMEM (Thermo Fisher cat# A1896701) with 10% tetracycline-free FBS was added. For live imaging, 20µM CCCP was added and images were acquired every two minutes at a 2h interval.

Analysis of mitochondrial membrane potential

Glucose and galactose-grown U2OSn ataxin-3 KO GFP-Parkin cells were seeded in a four-chamber dish (Greiner cat# 627870) with 70,000 cells 24h before. The next day cells were treated with 20nM of tetramethylrhodamine, methyl ester (TMRM) (Thermo Fisher cat# T668) and incubated for 30 minutes, then washed with fresh corresponding DMEM, and imaged under the Zeiss live imaging microscope using the 20x objective with Alexa 488 and mCherry channels for acquisition.

Cell cycle analysis

HEK293T and U2OSn ataxin-3 KO cells were dissociated by trypsinization, spun down, washed twice with PBS, and the cell pellet was then fixed in cold 70% ethanol for 30 minutes. The cells were collected, centrifuged and washed once with PBS, and then treated with RNase suspended in PBS, including 0.1% Triton X-100 and 1% BSA for 20 minutes at room

temperature, followed by incubation with 5µl of propidium iodide (PI) for 30 minutes. Next, PBS was added to stop the action of PI, and cell cycle distribution was analyzed on the Attune™ NxT flow cytometer (Thermo Fisher).

Determination of the rate of cell proliferation

HEK293T ataxin-3 KOs and wildtype cells were seeded onto a 6-well plate in duplicates and placed on the JuLI live cell imaging system (by NanoEnTek Inc) housed within an 5% CO_2 incubator at 37°C. Brightfield images covering 3 fields per well were established with continuous acquisition every 2 minutes and a time-lapse imaging was performed over 35h. To observe cell proliferation, the change in cell surface area over time was measured using CellProfiler™ software (BROAD Institute) and the Columbus™ analyzer system (PerkinElmer). The imaging analyzer receives the raw image, finds colony edges in order to determine the cell area, and then creates a mask and filter of the colony areas in the well. After data acquisition is complete, changes in cell surface area over time were analyzed and compared between each hour, each field, and each well.

Mitochondrial turnover assay

A mitochondria-targeted (mt)-Keima assay was done to quantify mitochondria turnover in U2OSn ataxin-3 KO GFP-Parkin cells. The pFB-ERV vector (Agilent plasmid #217564) and mt-Keima plasmid (a gift from A. Miyawaki, Laboratory for Cell Function and Dynamics, Brain Science Institute, RIKEN, Japan) were transiently transfected using the JetPRIME® protocol on 200,000 cells seeded in a 6-well plate. Ponasterone A (Abcam ab144330) was added 24h later to

induce production of the mt-Keima protein and allow for selection of cells with the plasmid. The next day, 20μM CCCP was added for 4h before FACS analysis. The Attune™ NxT flow cytometer was used to measure the results of this assay.

Statistical Analysis

For statistical analyses, one-way ANOVA followed by a Dunnett's test, and a two-way ANOVA followed by a Tukey test was performed using Graph Pad Prism 8.0 (La Jolla, CA). Data was obtained from the indicated number of experiments and findings were considered significant as follows: *P < 0.05, **P < 0.01, ***P < 0.001, ****P < 0.0001, ns P > 05; mean + SEM. Graphs were produced using Graph Pad Prism version 8.0 and Excel.

Results

CRISPR knockout of ataxin-3 in cultured cells

The purpose of a gene knockout (KO) is to abolish the expression of that gene within the cell to elucidate what effect its absence might have on distinct molecular cellular processes. The CRISPR/Cas9 technique [80] has become a powerful tool in genome-editing due to its ease of use and was the preferred tool to use for this project to KO ataxin-3. To knockout the *ATXN3* gene using CRISPR, a guide RNA (gRNA) containing a combination of two molecules: one scaffold sequence to bind to Cas9 protein, and another user-defined sequence that binds to a target specific DNA region was designed. In this research, a two-gRNA strategy [81] was used to remove exon 2 of *ATXN3* to create a frameshift, leading to a premature stop codon that prevented the expression of the protein **(Figure 4)**. This is an effective way to disrupt gene function in a cell because the transcript is targeted for degradation and ensuring the functional protein is never translated [82].

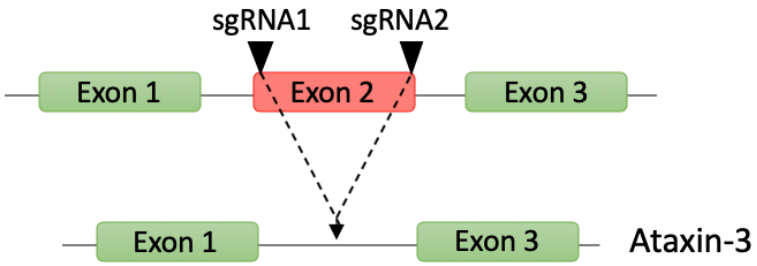

Figure 4. CRISPR KO strategy.
Workflow in HEK293T and U2OS cells for targeting exon 2 removal of ataxin-3 using a two-gRNA tactic.

HEK293T cells and U2OSn cells were used for the generation of these KO cell lines. Genomic DNA of clones were harvested for DNA amplification by PCR, to confirm whether the *ATXN3* sequence was disrupted and a KO had occurred. Out of 20 positive clones, five were

selected for expansion into stable HEK293T ataxin-3 KO cell lines and four clones were selected for U2OSn ataxin-3 KO cell lines. These HEK392T ataxin-3 KO cell lines were generated as tools to be used for further multiple cell and molecular biology applications. The U2OS ataxin-3 KO cell lines were generated in order to have cells suitable for imaging methods, such as immunofluorescence (IF), confocal imaging, and live cell imaging, as U2OS are bigger cells and easier to image relative to HEK293T cells. After genomic DNA extraction, sequencing of the KO cells revealed a complete removal of exon 2 in both HEK293T (**Figure 5A**) and U2OSn cell types (**Figure 5B**). Additionally, for HEK293T clones, there were two different deletions detected in the exon: an 81bp deletion for 3 clones (KO 1, 3, 4) showing a truncated non-functional protein, and an 80bp deletion in 2 clones (KO 2, 5) creating a frameshift and leading to two in frame stop codon insertions; both deletions still demonstrated a true KO of ataxin-3.

A. HEK293T SnapGene Genomic Sequence

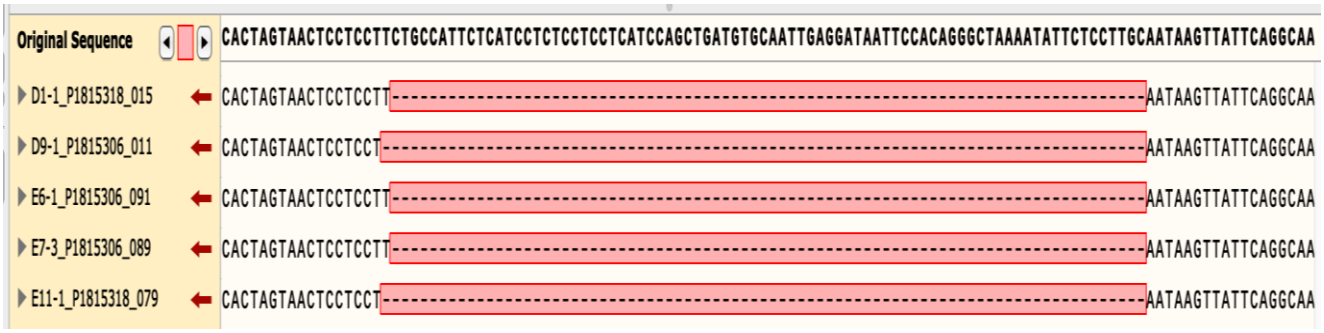

Figure 5A. HEK293T genomic sequence with *ATXN3* exon 2 removal.

Legend

D1-1 = KO 1

D9-1 = KO 2

E6-1 = KO 3

E7-3 = KO4

E11-1 = KO5

Original sequence = HEK293T wildtype

B. U2OSn SnapGene Genomic Sequence

<u>Figure 5B.</u> U2OSn genomic sequences following the CRISPR-mediated removal of exon 2 in *ATXN3*.

<u>Legend</u>

KO1-1F = KO 1

KO2_A1 = KO 2

KO3-1F = KO 3

KO4-1F = KO4

WT-1F = U2OSn wildtype

Characterization and validation of ataxin-3 knockout lines

Once both HEK293T and U2OSn ataxin-3 KO cell lines were generated, a characterization and validation process were performed to confirm that the ataxin-3 protein was no longer expressed using immunoblotting and immunofluorescence application.

Antibody validation for WB

Along with cell line characterization, it was equally important to identify reliable and validated antibodies. The criteria for choosing appropriate antibodies was based on the recent antibody characterization process of Laflamme and colleagues [83], where a pipeline was created to characterize antibodies already on the market in order to ensure antibodies were validated and consistent for research use. According to their criteria, one must: 1) identify high expressing cell lines with the protein of choice that are readily modifiable by CRISPR/Cas9, 2) generate a KO in this cell line and sequence validate, 3) find all available commercial antibodies that target the protein of interest and 4) screen all antibodies by immunoblot with multiple cells lines of the KO and parental line, in order to identify highest expressing cell line(s), and lastly 5) use selected edited cell line to screen antibodies for specificity by IF and immunoprecipitation [83]. After following step 1 and 2 of this pipeline, the next step was to find suitable commercially available antibodies. A total of five antibodies: two monoclonal and three polyclonal antibodies were chosen from different companies and all came from different clones*. A schematic of ataxin-3 domain depicting where each antibody binds to its specific epitope is shown (**Figure 6**).

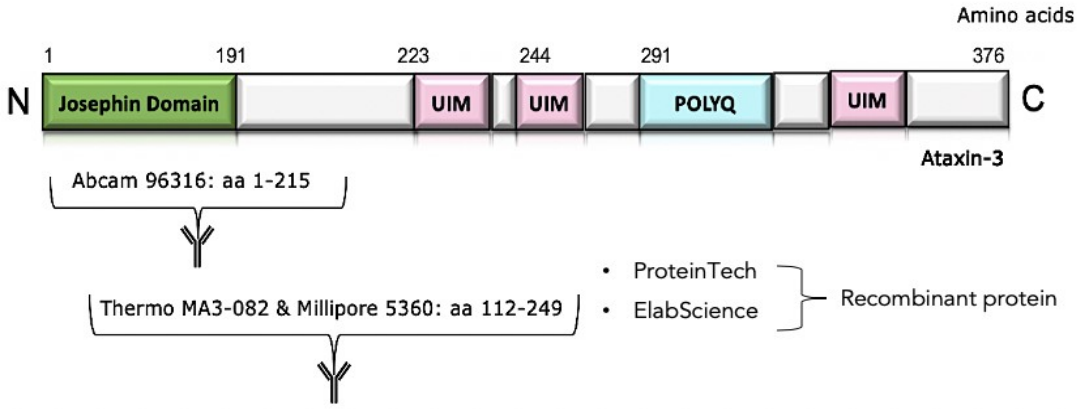

Figure 6. Antibody epitope binding to ataxin-3.
Ataxin-3 schematic showing its amino acids and the epitope of where each antibody binds to. Expectedly, only monoclonal antibodies show the precise location of ataxin-3 binding.

The candidate antibodies were Millipore MAB5360 mouse monoclonal 1H9, Thermo Fisher MA3-082 mouse monoclonal, ProteinTech #13505-1-AP rabbit polyclonal, ElabScience E-AB-60279 rabbit polyclonal, and Abcam ab96316 rabbit polyclonal. All antibodies were screened by WB using the five HEK293T and four U2OSn ataxin-3 KO clones plus their respective parental cell lines. All antibodies were used in 1:1000 dilution.

To confirm loss of protein expression in both cell lines, all five antibodies were screened, and WBs were done on the selected clones for each cell line, with our results showing an ablation of ataxin-3 expression in our clones relative to the respective parental cell line (**Figure 7**). Specifically, Millipore MAB5360 and Thermo Fisher MA3-082 best demonstrated a clear and strong signal in the parental HEK293T lysates and no signal was detected for the five KO lines compared to two bands in the wildtype cells which most likely represents proteins translated from the two endogenous *ATXN3* alleles. Additionally, no band other than ataxin-3 is visible. The other antibodies also gave specific signals for ataxin-3, but there were many other non-specific bands detected on the blots. The same perception applies for U2OSn wildtype and KO lines, but the signal is not as strong as HEK293T. From these findings, we concluded that our clones have abolished protein expression and MAB5360 meets the criteria for validation, and this became the validated antibody that we continued using for WB applications and determining ataxin-3 levels.

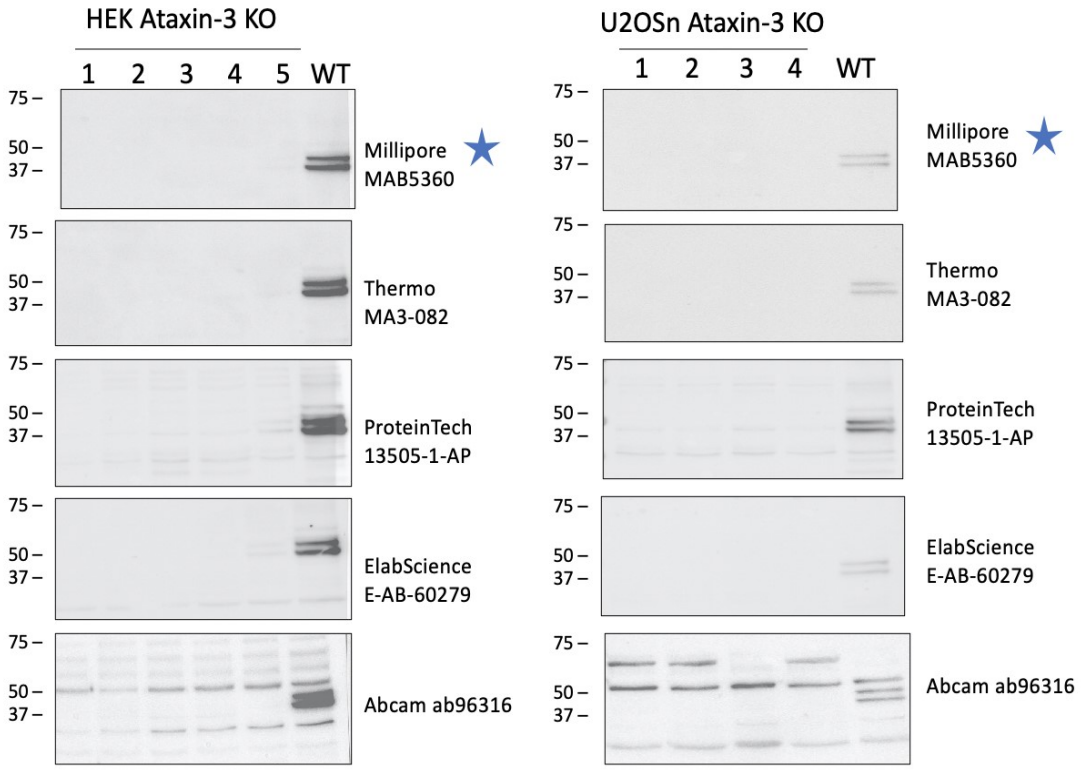

Figure 7. Ataxin-3 antibody validation via immunoblot.
Western Blot of all screened antibodies depicting the ataxin-3 protein binding and specificity on (**A**) HEK293T ataxin-3 KOs and (**B**) U2OSn ataxin-3 KOs with respective wildtype.

Antibody validation for IF

Since the U2OSn ataxin-3 KO cell lines were generated to facilitate imaging studies given its larger cell size and shape, the next step was to test the efficacy of the antibodies for IF applications. The mosaic approach for the antibody validation was the imaging workflow used, as described by Laflamme and colleagues [83]. This strategy involved transiently transfecting the parental cell line with a GFP vector and the ataxin-3 KO cell line with an RFP vector. Wildtype GFP and KO RFP cells were plated on the same coverslip, seen on **Figure 8A**, and each cell type could be distinguished based on their fluorescence, giving a mosaic look under the microscope.

This approach reduces microscopic imaging and figure analysis biases, giving optimal results. The primary antibodies were diluted 1:1000, and all five antibodies were screened using the mosaic strategy. In the coverslip, there are sometimes a few overlapping cells, so the principle was to image dispersed individual GFP and RFP cells next to each other to detect their true fluorescent signal for each cell. Under the microscope, a true wildtype has GFP-only signal and there is no other background stain, whereas a true KO cell has RFP-only signal. After screening all antibodies, it was found that ProteinTech #13505-1-AP was the only antibody to specifically recognize ataxin-3. All the other antibodies generated non-specific staining that was comparable between the parental and KO cells. This showed that ProteinTech #13505-1-AP had a potential to be a specific antibody for IF, as summarized in **Figure 8B**. ProteinTech #13505-1-AP is specific to ataxin-3 because in the wildtype, there is a strong nuclear and dispersed cytoplasmic fluorescent signal in the cells that is significantly reduced in the KO cell (**Figure 8C**).

8A

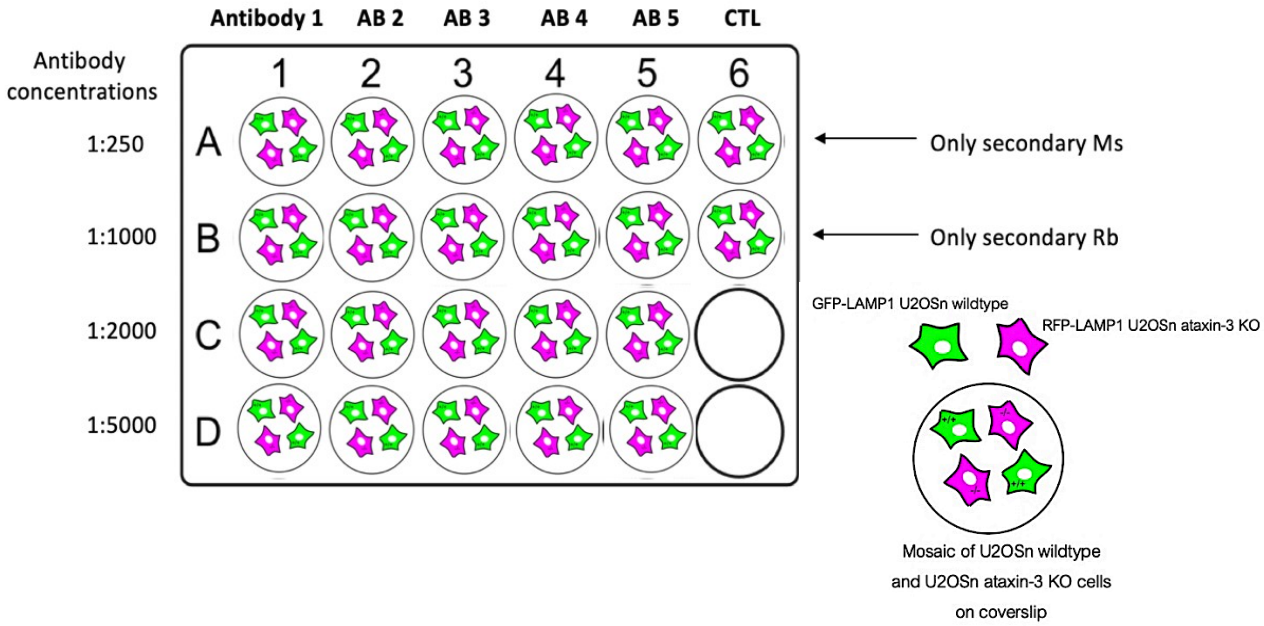

8B

Antibody	**Clone ID**	**Species**	**Dilution**	**Specificity**
Abcam 96316	Polyclonal	Rabbit	1:1,000	Nonspecific
Thermo Fisher MA3-082	2SCA-1H9	Mouse	1:1,000	Nonspecific
Millipore MAB5360	1H9	Mouse	1:1,000	Nonspecific
ProteinTech 13505-1-AP	Polyclonal	Rabbit	1:1,000	**Specific**
ElabScience E-AB-60279	Polyclonal	Rabbit	1:1,000	Nonspecific

8C

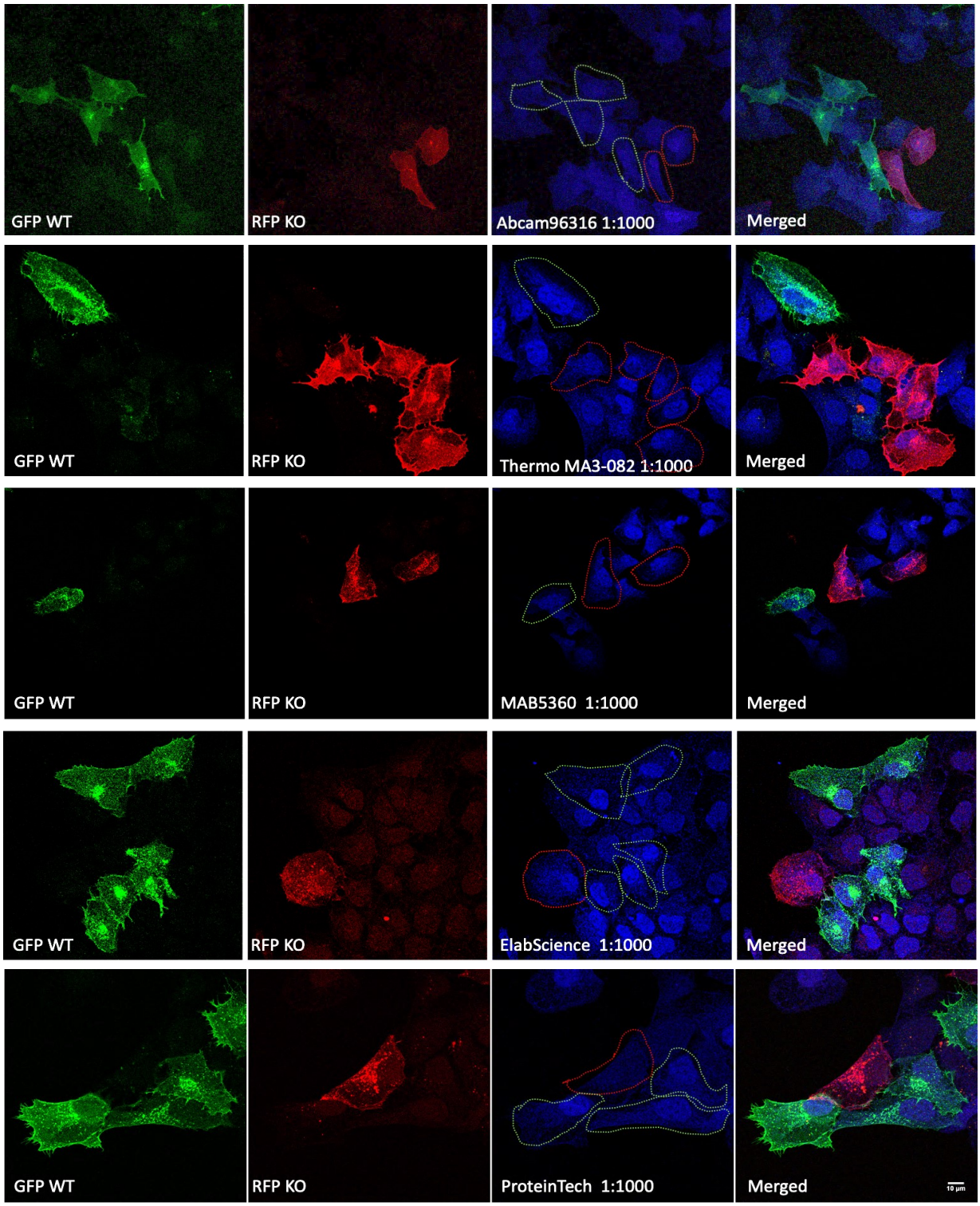

<u>Figure 8.</u> IF strategy for antibody validation.

(**A**) Mosaic strategy of wildtype GFP and KO RFP in coverslips on a 24-well plate with all five antibodies using different dilutions and two controls for each host (**B**) Summary of all antibodies, its clone, host species, tested dilution, and specificity for ataxin-3 protein (**C**) IF demonstrating ataxin-3 specificity of all candidate antibodies, where the wildtype GFP is circled in green and the RFP KO is circled in red when staining for ataxin-3 (blue).

After this first screen, ProteinTech #13505-1-AP was tested with several dilutions to analyze its specificity and determine an ideal dilution for best results. Dilution series were tested from 1:200 – 1:20,000. For all the dilutions tested, except 1:200, the antibody signal was specific with the strong nuclear and dispersed cytoplasmic signal in the wildtype, and the KO showing a largely reduced signal of the nucleus, cytoplasm and absent mitochondrial staining (**Figure 9**), and the results are summarized in **Table 2**. Thorough microscopic observations determining the subcellular staining was as expected from the control condition, it demonstrated that ProteinTech #13505-1-AP gave a specific signal and therefore met validation criteria for IF applications at recognizing endogenous ataxin-3. With fully validated antibodies for WB and IF applications, it was possible to effectively characterize and validate both HEK293T and U2OSn ataxin-3 KO cell lines. Although the mutagenesis made with CRISPR/Cas9 approach is checked by DNA sequencing, the true validation is the absence of protein being expressed in cells, and this is what requires having a validated antibody. In this project, the validation of a KO was determined by the absence of a molecule, and thanks to this validation pipeline, it ensured that a real ataxin-3 and true KO signal was observed in all experiments.

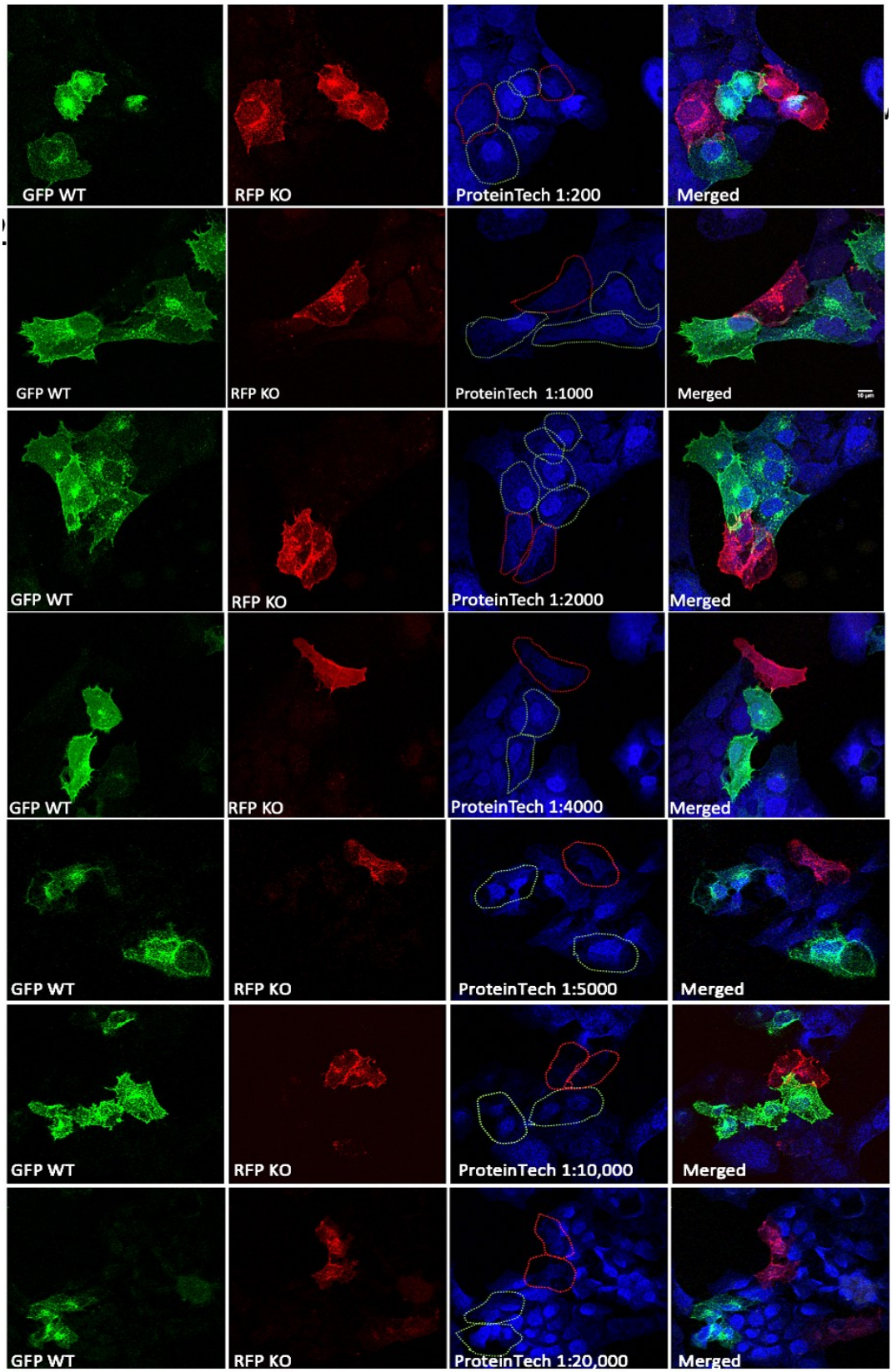

Figure 9. ProteinTech dilution series on IF.
Confocal imaging of dilution series of ProteinTech antibody representing specific or nonspecific signal of ataxin-3 (blue), where the KO is circled in red and WT is circled in green.

ProteinTech 13505-1-AP Dilutions	Specific?
1:200	No
1:1,000	Yes
1:2,000	Yes
1:4,000	Yes
1:5,000	Yes
1:10,000	Yes
1:20,000	Yes

Table 2. ProteinTech antibody dilution.
Range of dilution series in IF to detect specificity of the antibody. All dilutions were specific except for the most concentrated.

Measuring effects on cell proliferation and cell cycle timing

In order to understand what happens in the cell when ataxin-3 is absent, measuring cell viability and evaluating how healthy the cells are in both cell lines was important since ataxin-3 has been implicated in cell quality control and cytoskeletal organization [2, 37, 40, 84, 85]. To measure cell cycle timing in HEK293T and U2OSn ataxin-3 KOs, propidium iodide (PI) was used to analyze this activity. PI is a fluorescent agent used to stain DNA to evaluate the cell viability and determines how the cells are distributed with respect to the cell cycle stages. The treatment with PI demonstrated that the absence of ataxin-3 had no effect on cell cycle, as all cell lines were mostly in a G1 growth phase, and cell viability seemed to be steady, similar to wildtype HEK293T and U2OSn cell lines (**Figure 10).**

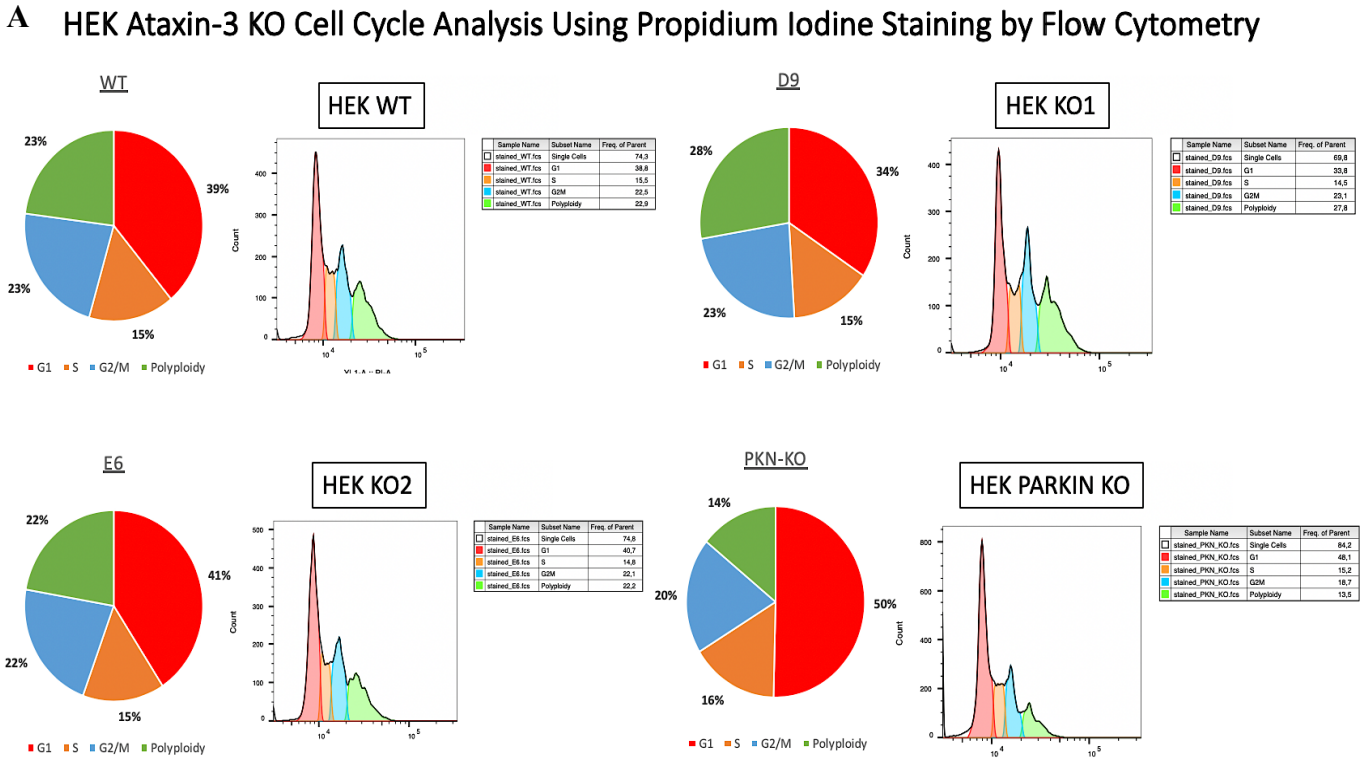

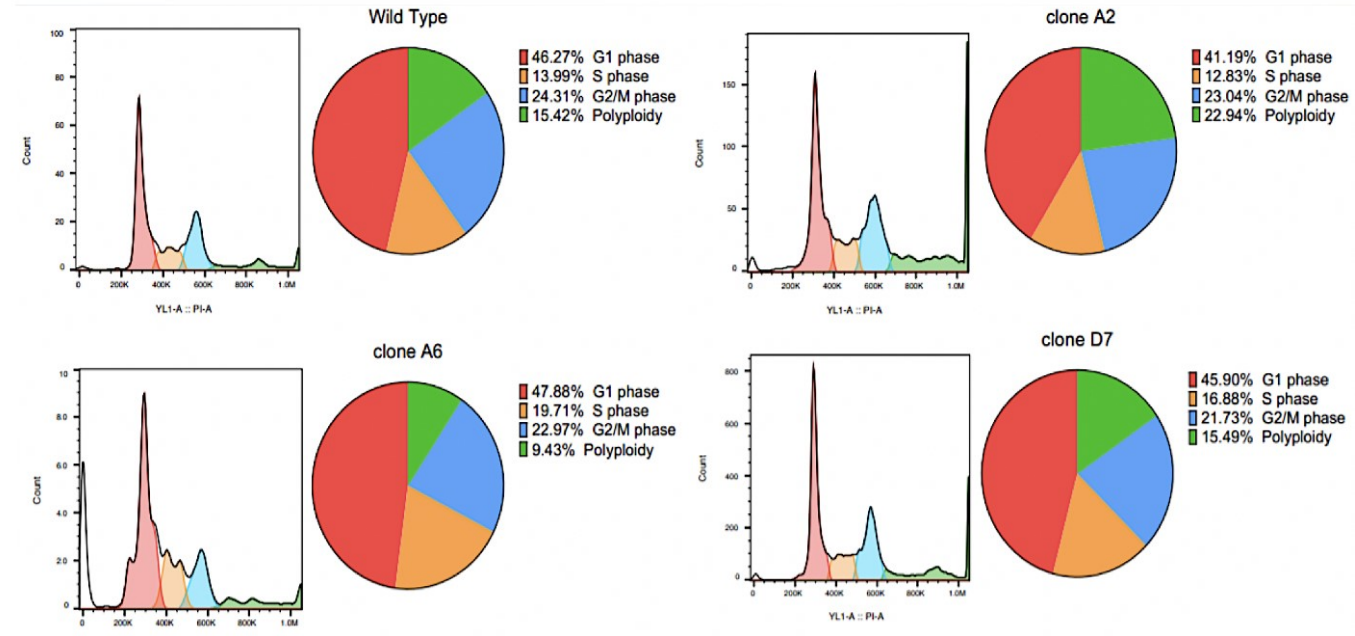

Figure 10. Cell cycle analysis using propidium iodide staining by flow cytometry.

Propidium iodide staining on (**A**) HEK293T ataxin-3 KO cells and (**B**) U2OSn ataxin-3 KO cells revealed no effect on cell cycle timing when ataxin-3 was removed from these cell lines compared to the wildtype cells.

Furthermore, to see if there were differences in cell proliferation between wildtype and ataxin-3 KO cells, cells were imaged by time-lapse microscopy on the JuLI™ Imaging System, a real-time cell history recorder that enables image capturing and preparation of time-lapse movies. HEK293T and U2OSn ataxin-3 KOs and respective wildtype cells were placed on the JuLI™ live cell imaging system and brightfield images covering 3 fields per well were established with continuous acquisition and time-lapse imaging over 35h. To observe cell proliferation, changes in cell surface area over time was measured. For the analysis, edges of the cell colonies were defined using the image analysis software, helping to determine the cell area. After data acquisition is complete, changes in cell surface area over time were analyzed and compared between each hour, each field, and each well. This is represented in the graph as an individual line for each sample, showing for each cell line the dynamic raw data input. Quantitative graphs of cell proliferation analysis showed that HEK293T wildtype (green lines) proliferated and spread slightly better than the two ataxin-3 KOs (dark blue lines and light blue lines for respective KO) starting at 24h until 30h for KO1, and 30h until the end of the 35h time-interval for both ataxin-3 KOs **(Figure 11A)**. However, no significant difference of cell proliferation for the U2OSn wildtype cells (green lines) was seen compared to three ataxin-3 KOs (dark, medium and light blue lines) (**Figure 11B**).

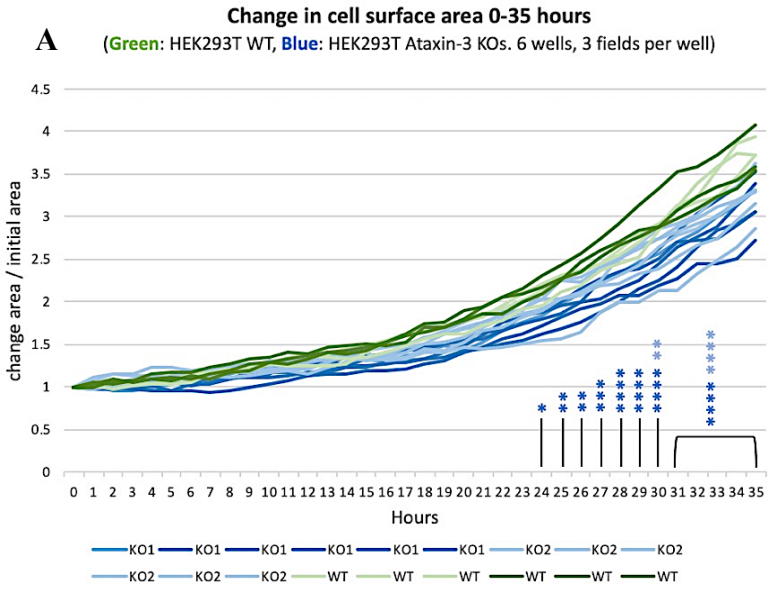

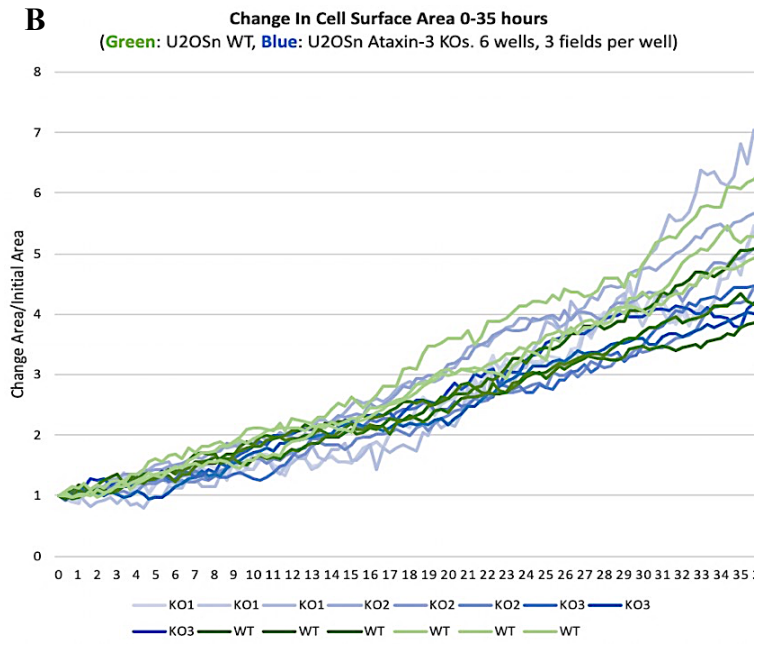

<u>Figure 11.</u> Cell proliferation assay on HEK293T and U2OSn ataxin-3 KO cells.

Cell proliferation assay demonstrated significant proliferation difference in wildtype than two ataxin-3 KOs in **(A)** HEK293T cells compared to wildtype and three ataxin-3 KOs in **(B)** U2OSn cells which showed no alteration in proliferating cells in culture over a 35hr time-interval.

A two-way ANOVA was used with *P < 0.05, **P < 0.01, ***P < 0.001, ****P < 0.0001, ns P > 0.05; n = 1, mean + SEM.

Significance of color scheme depicts how wildtype is significantly different from KO 1 (dark blue) and KO 2 (light blue) asterisk and legend colors in HEK293T cells.

In summary, both the PI experiment observing cell cycle behavior, and cell proliferation time-interval measurement in the JuLI System determined that when ataxin-3 is absent, no overt alterations or defects with the cells when ataxin-3 was detected, and KO cells appeared to be

sustainable and healthy. However, there was a significant difference in the cell proliferation trend in HEK293T cells that might have impact on growth in the absence of ataxin-3.

Observing the effect on parkin stability

In order to first look at baseline levels of parkin in ataxin-3-depleted cells, HEK293T ataxin-3 KO cell lysates were loaded on a 10% SDS-PAGE gel. Blots revealed normal amount of parkin levels in the KOs and wildtype (**Figure 12A**). There was some variability of parkin levels seen in HEK293T ataxin-3 KO 2 cells, but this could be inter-clone variability in terms of parkin expression or simply just outliers compared to the other findings since the majority of KOs have levels of parkin equivalent to the parental line. Overall results showed there is no difference in parkin levels in HEK293T cells lines in the absence of ataxin-3. For a more quantitative approach, HEK293T ataxin-3 KO cells were lysed, and parkin and ataxin-3 levels observed with the LI-COR Odyssey 9120 Imaging System and total protein stain. LI-COR WB results showed that there were also no differences in parkin level between KOs and wildtype cells (**Figure 12B**). Additionally, ataxin-3 levels were examined in HEK293T parkin KO cells to see if there was a correlation between the protein levels of both proteins. WB of HEK293T parkin KO cell lines blotted for ataxin-3 showed that there was no difference in ataxin-3 levels compared to wildtype (**Figure 12C**). These results were expected, and this implies that when either protein is absent, the levels of the observed protein is not affected and therefore ataxin-3 and parkin do not appear to regulate the stability of each other.

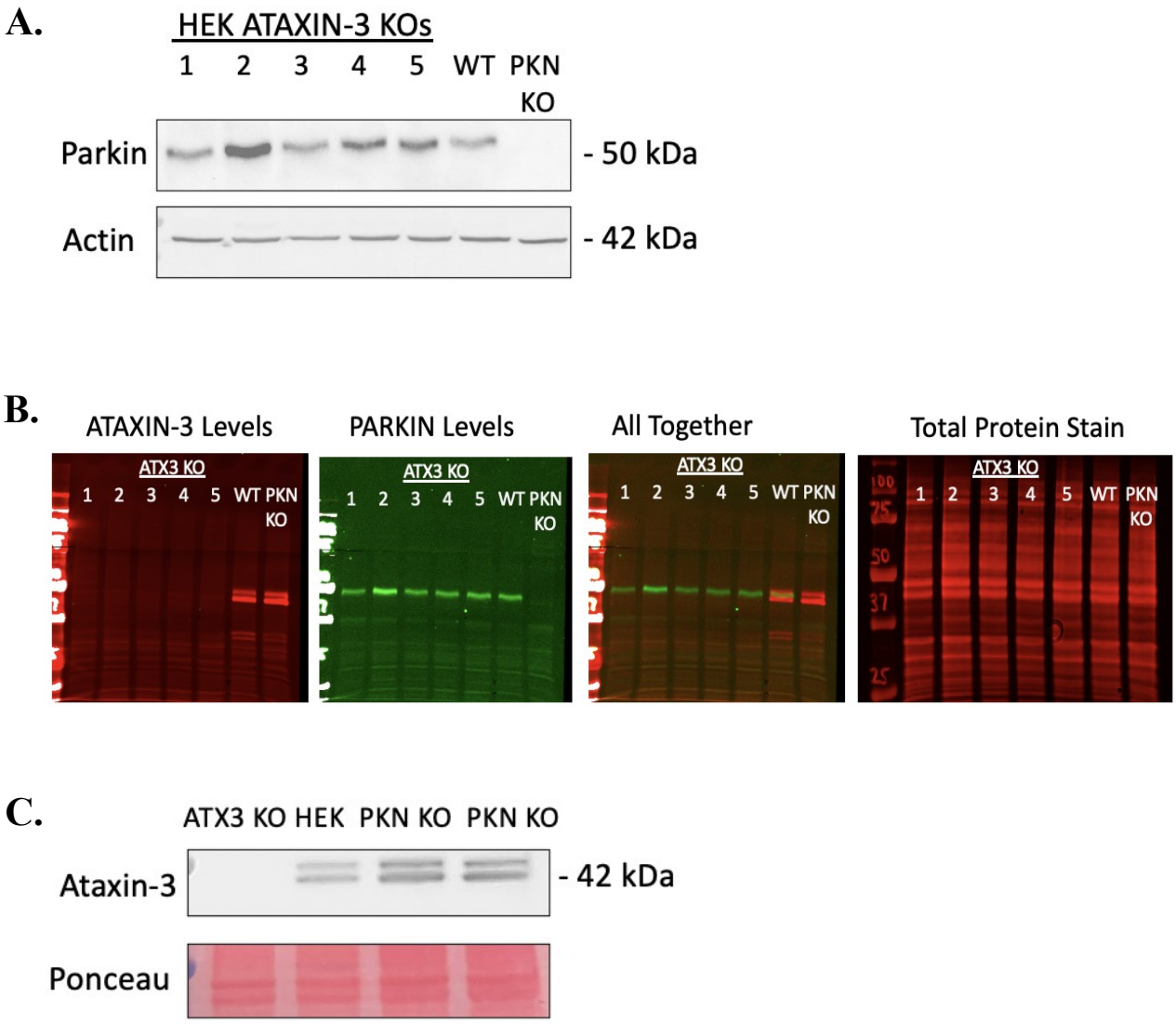

Figure 12. Biochemical assays observing ataxin-3 and parkin levels

(A) Western Blot showing parkin levels in HEK293T ataxin-3 KOs along with their loading control in a standard immunoblot. (**B**) LI-COR Odyssey quantitative immunoblot technique showing parkin and ataxin-3 levels in HEK293T ataxin-3 KOs along with the total protein stain within the membrane. (**C**) Western Blot of Ataxin-3 levels in HEK293T wildtype and duplicated HEK parkin KOs along with ponceau to show proteins present in the membrane.

Investigating parkin function in the mitophagy pathway

Generation of GFP-Parkin line using U2OSn ataxin-3 KO

To study mitochondrial function and co-localization with parkin, wildtype U2OSn and ataxin-3 KO cells were transfected with a pEGFP-Parkin WT vector and later selected using G418 for 10 days in order to create a stable cell line. FACS analysis on the generation of this GFP-Parkin cell line showed that all KO cell lines plus wildtype cells were effectively sorted for GFP-positive cells and were expanded in culture for all future experiments (**Figure 13**).

A.

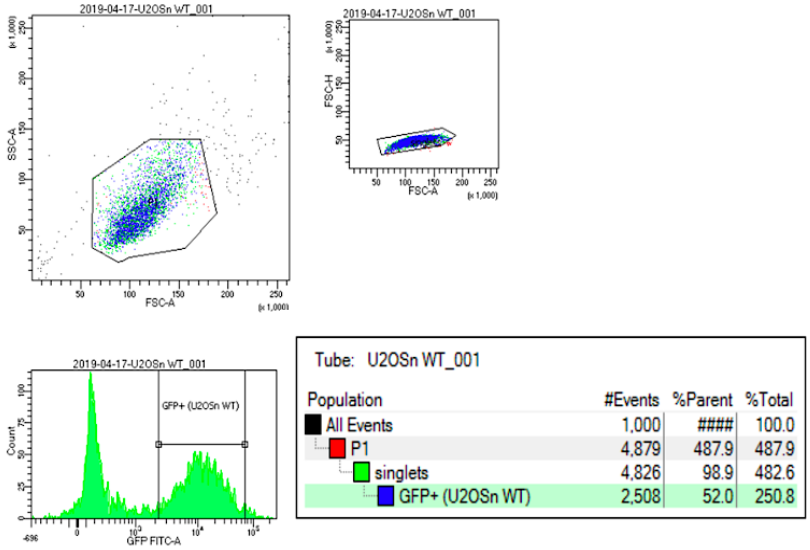

B.

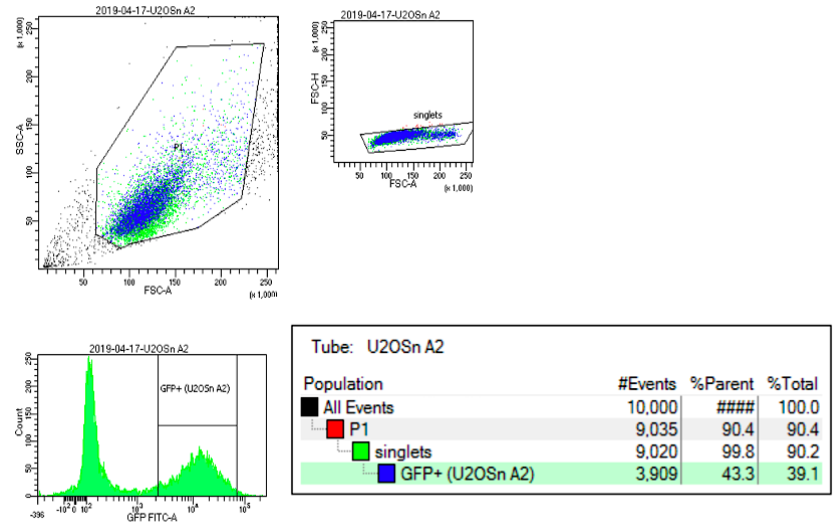

Figure 13. Generation of U2OSn ataxin-3 GFP-Parkin cell line. FACS report of the GFP-positive cells that were sorted for each cell line. Showing an example of report for (**A**) U2OSn wildtype cells with 52% GFP-positive cells and (**B**) A2 which is KO1 of U2OSn ataxin-3 cells with 43.3% of GFP-positive cells that were recovered and placed in culture to expand, use for experiments, and freeze as backups.

Moreover, in order to further study mitochondrial function in ataxin-3 depleted cells, wildtype and U2OSn ataxin-3 KO GFP-Parkin cell lines were changed from being in high glucose DMEM to galactose media. This was done to promote mitochondrial function through the electron transport chain (ETC). When cells are cultured in high glucose DMEM, it is difficult to study mitochondrial (dys)function as ATP production primarily proceeds via the glycolysis pathway. Rather, catabolized by the pentose phosphate pathway, galactose is known to enhance mitochondrial metabolism as it forces the cells to have an increased dependence on oxidative phosphorylation through the ETC for ATP production, thus it is a good model to study specific mitochondrial functions [86].

Measuring mitochondrial membrane potential

To observe the state of the mitochondria activity, specifically the mitochondrial membrane potential in the absence of ataxin-3, both glucose and galactose U2OSn ataxin-3 KO GFP-Parkin cells were treated with 20nM of TMRM, a cell permeable red dye that accumulates in active mitochondria with undamaged membrane potential. Thus, if the cells have healthy mitochondria, the red signal will be bright compared to an absence of signal when the mitochondria have become depolarized, losing their active membrane potential. The comparison of mitochondrial membrane potential between glucose and galactose-grown cells showed that there was no significant difference in high glycolytic cells compared to galactose cells (**Figure 14A**), which shows a striking decrease of potential in the wildtype. More importantly, ataxin-3

KOs had an increased mitochondrial potential relative to the wildtype in galactose-grown cells (**Figure 14B**).

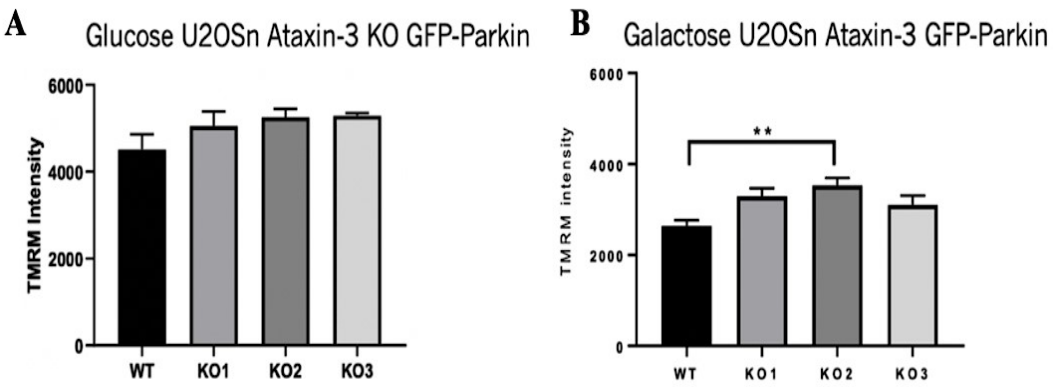

Figure 14. TMRM intensity in glucose/galactose-grown U2OSn ataxin-3 KO GFP-Parkin cells.
Mitochondrial membrane potential observation on (**A**) glucose-grown cells show there is no significant difference in potential intensity when ataxin-3 is absent compared to (**B**) galactose-grown cells where the potential is increased in the KOs compared to the wildtype. An ordinary one-way ANOVA was used with *P < 0.05, **P < 0.01, ***P < 0.001, ****P < 0.0001, ns P > 0.05; n = 3, mean + SEM.

Measuring parkin recruitment using CCCP

In cultured cells, parkin pathways can be activated by depolarizing mitochondria with uncouplers such as carbonyl CCCP. Following CCCP treatment, parkin usually shows a robust recruitment to mitochondria after 2h, which is then followed by the clearance of mitochondria, also known as parkin-mediated mitophagy [63]. To measure this activity, U2OSn ataxin-3 KO GFP-Parkin cells were treated with 20μM CCCP for 0h, 2h, 4h, and 6h, and then observed under the confocal microscope. Confocal microscopy results revealed that parkin recruitment did not seem to be altered in ataxin-3 KO cells, regardless of the time interval (**Figure 15**).

A. CCCP Treatment of Wildtype U2OSn GFP- Parkin

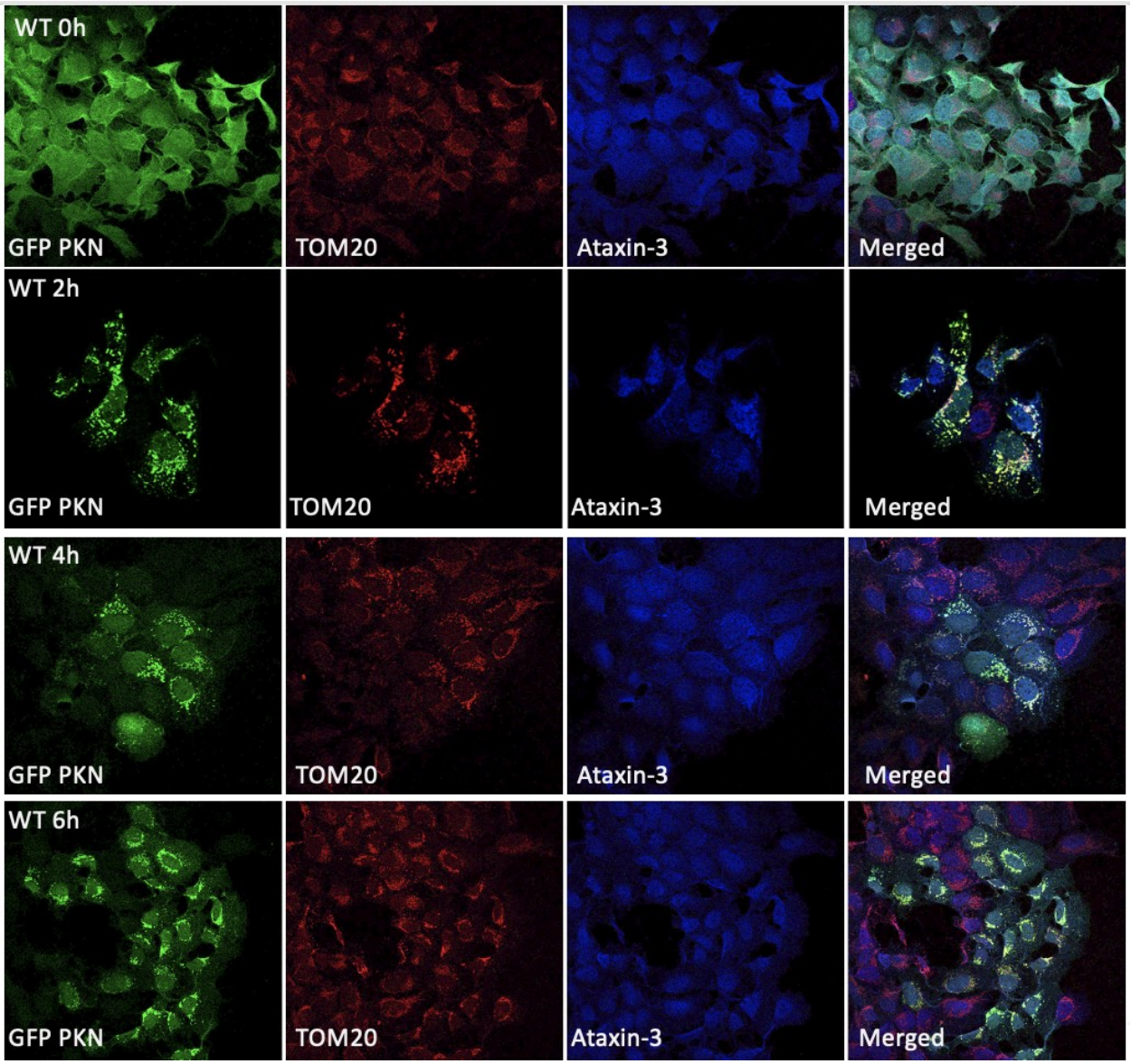

B. **CCCP Treatment of U2OSn Ataxin-3 KO GFP- Parkin**

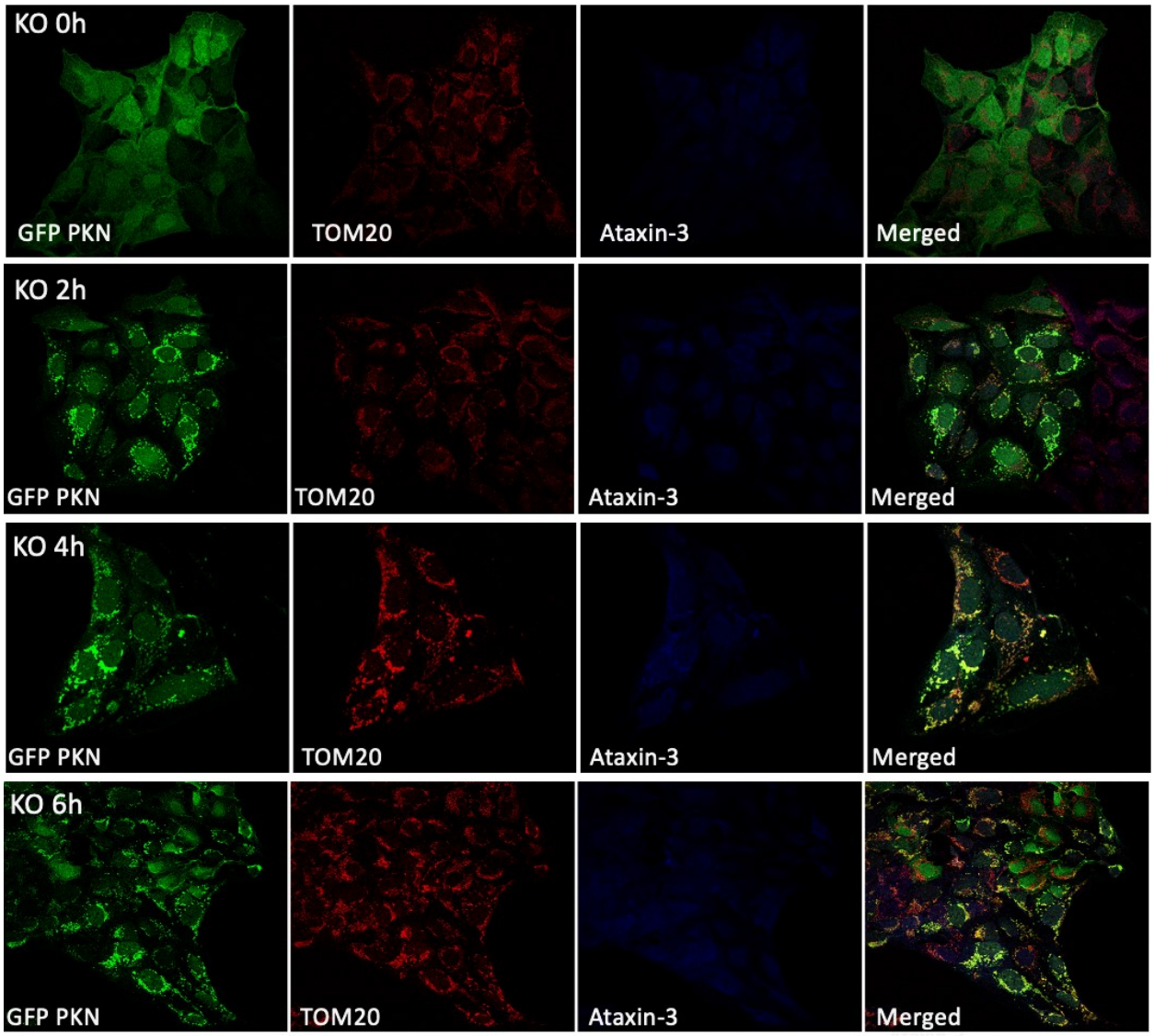

Figure 15. IF of U2OSn ataxin-3 KO GFP-Parkin CCCP treated cells.
Confocal imaging showing parkin recruitment (green), TOM20 (red) and ataxin-3 (blue) in CCCP-treated (**A**) U2OSn GFP-Parkin wildtype cells and (**B**) U2OSn ataxin-3 KO GFP-Parkin cells. Parkin recruitment is seen in both cell lines with no difference on recruitment over time.

To quantify CCCP parkin recruitment and see if there were indeed no differences in parkin recruitment, the same treatment and a 1h time interval was tested using Zeiss live imaging microscopy. For additional comparisons, cells grown in galactose also went through this CCCP treatment to see if there was a difference in recruitment compared to cells grown in glucose. Live imaging experiments showed a slightly reduced rate of recruitment in galactose-grown cells compared to glucose-grown cells, but overall no differences in parkin recruitment between wildtype and KO lines was observed in either cell type (**Figure 16**). Time interval movies captured parkin recruitment as puncta appeared over time and eventually vanished as mitochondrial was cleared. This reduced rate of recruitment for parkin in galactose media is consistent with data from McLelland and colleagues [66], where the mitochondrial translocation of parkin is also delayed in galactose-grown cells.

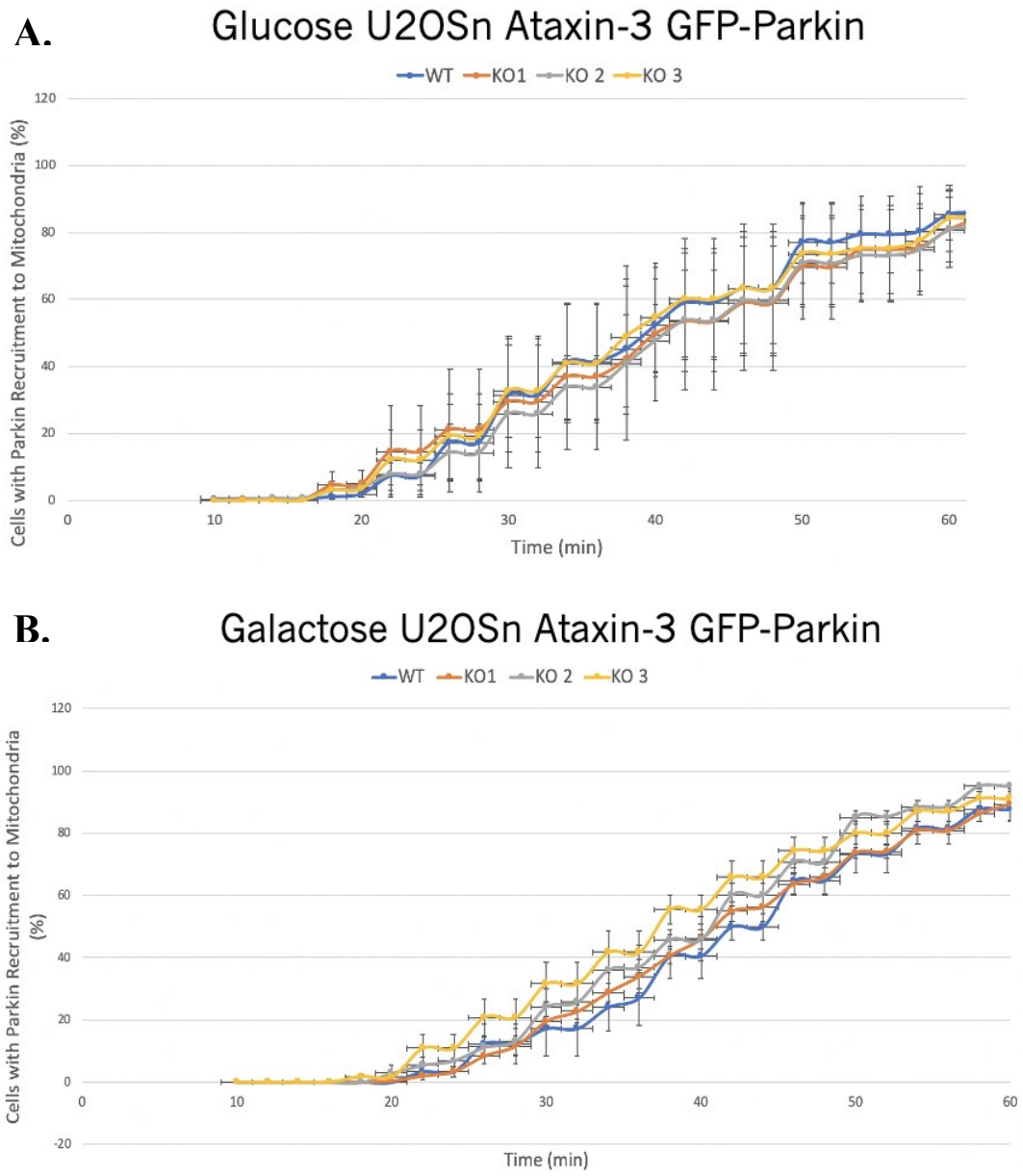

<u>Figure 16.</u> Zeiss live imaging of CCCP treated glucose/galactose-grown U2OSn ataxin-3 KO GFP-Parkin cells

CCCP treatment of glucose and galactose-grown U2OSn ataxin-3 KO GFP-Parkin cells to analyze parkin recruitment to mitochondria over 60 minutes. The respective quantitative representation of three independent experiments on (**A**) glucose cells show normal recruitment and no significant difference with the wildtype, compared to (**B**) galactose-grown cells which demonstrated a much slower parkin recruitment but also no significant difference in wildtype vs. ataxin-3 KO parkin recruitment. A two-way ANOVA was used with *P < 0.05, **P < 0.01, ***P < 0.001, ****P < 0.0001, ns P > 05; n = 3, mean + SEM.

Measuring parkin recruitment in the presence importazole

To be able to further assess the level of parkin recruitment, a second stressor was implemented. When antibody validation in ataxin-3 was being performed, ataxin-3 localization was also being examined in U2OSn cells. Multiple nuclear and cytoplasmic inhibitors were evaluated to confirm ataxin-3 location in the cell. Interestingly, mitochondrial parkin recruitment was detected after the nuclear inhibitor importazole was applied on U2OSn ataxin-3 KO GFP-Parkin cells. In cultured cells, importazole is a cell-permeable molecule that exclusively blocks importin-β-mediated nuclear import, without interrupting transportin-mediated nuclear import or CRM1-mediated nuclear export [87]. It transports cargo molecules with a nuclear localization signal into the nucleus, and it was intriguing that parkin was being recruited to the mitochondria in the presence of this nuclear inhibitor.

To look at parkin recruitment in the presence of importazole, U2OSn ataxin-3 KO GFP-Parkin cells treated with 40μM importazole for 0h, 2h, 4h, and 6h. Importazole-induced GPF-parkin distribution looked different from CCCP-recruited parkin, as GFP co-localized puncta were less dispersed and was not observed in all cells compared to CCCP. Overall, parkin recruitment was demonstrated in both wildtype and KO cells, and with no differences in recruitment between the cell lines (**Figure 17**).

However, although there was no change in mitochondrial parkin recruitment, the cell viability of importazole-treated cells was altered. Especially in ataxin-3 KO cells, after 4h or more of incubation with importazole, almost all ataxin-3 KO cells and some wildtype cells were dead. This project appears to be the first time that importazole was used to examine the location of ataxin-3 within cells. Accordingly, when analyzing IF confocal images in the wildtype U2OSn

GFP-Parkin cells, importazole does not appear to inhibit the nuclear localization of ataxin-3. In terms of cell viability, this is something interesting to further investigate.

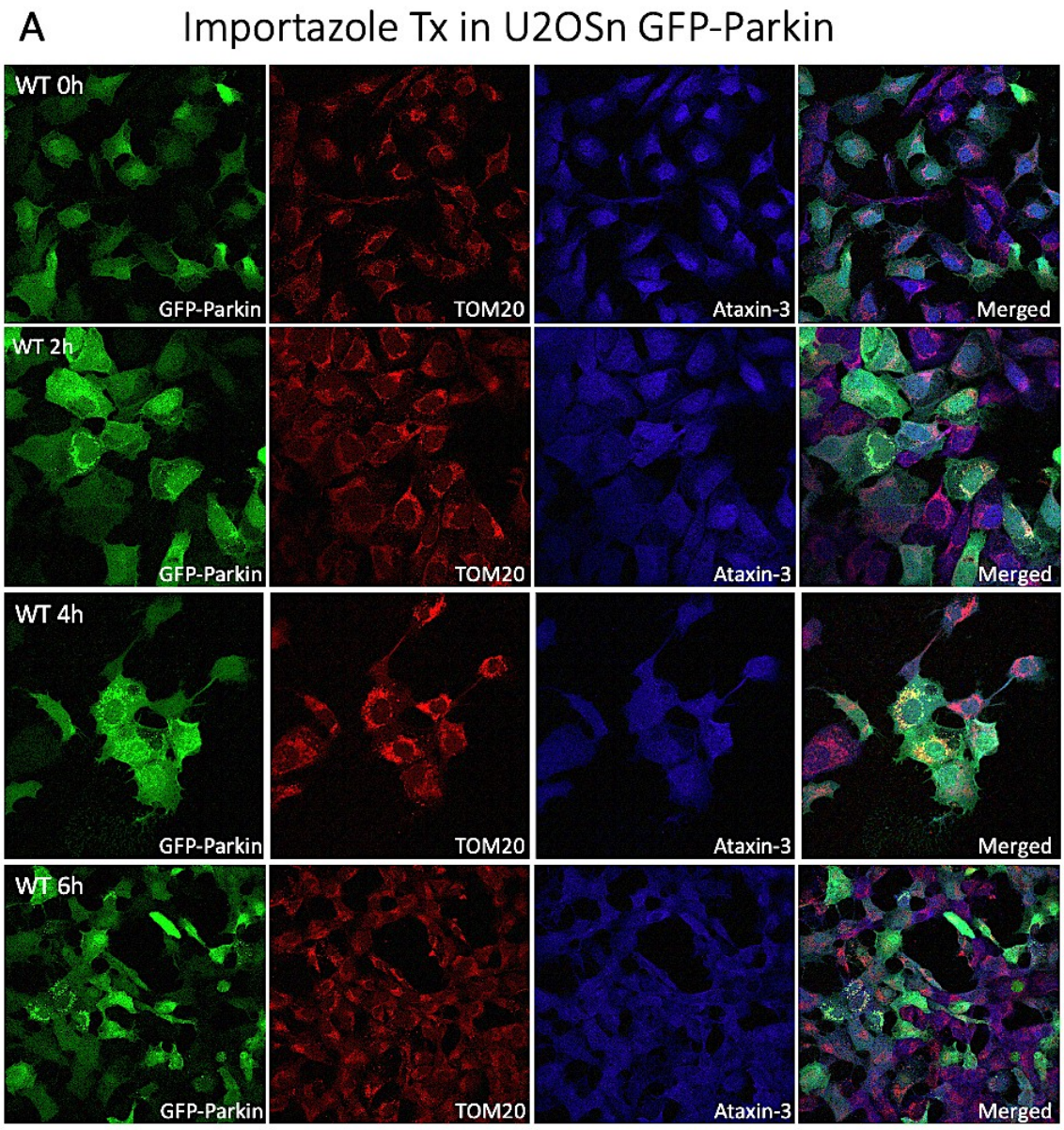

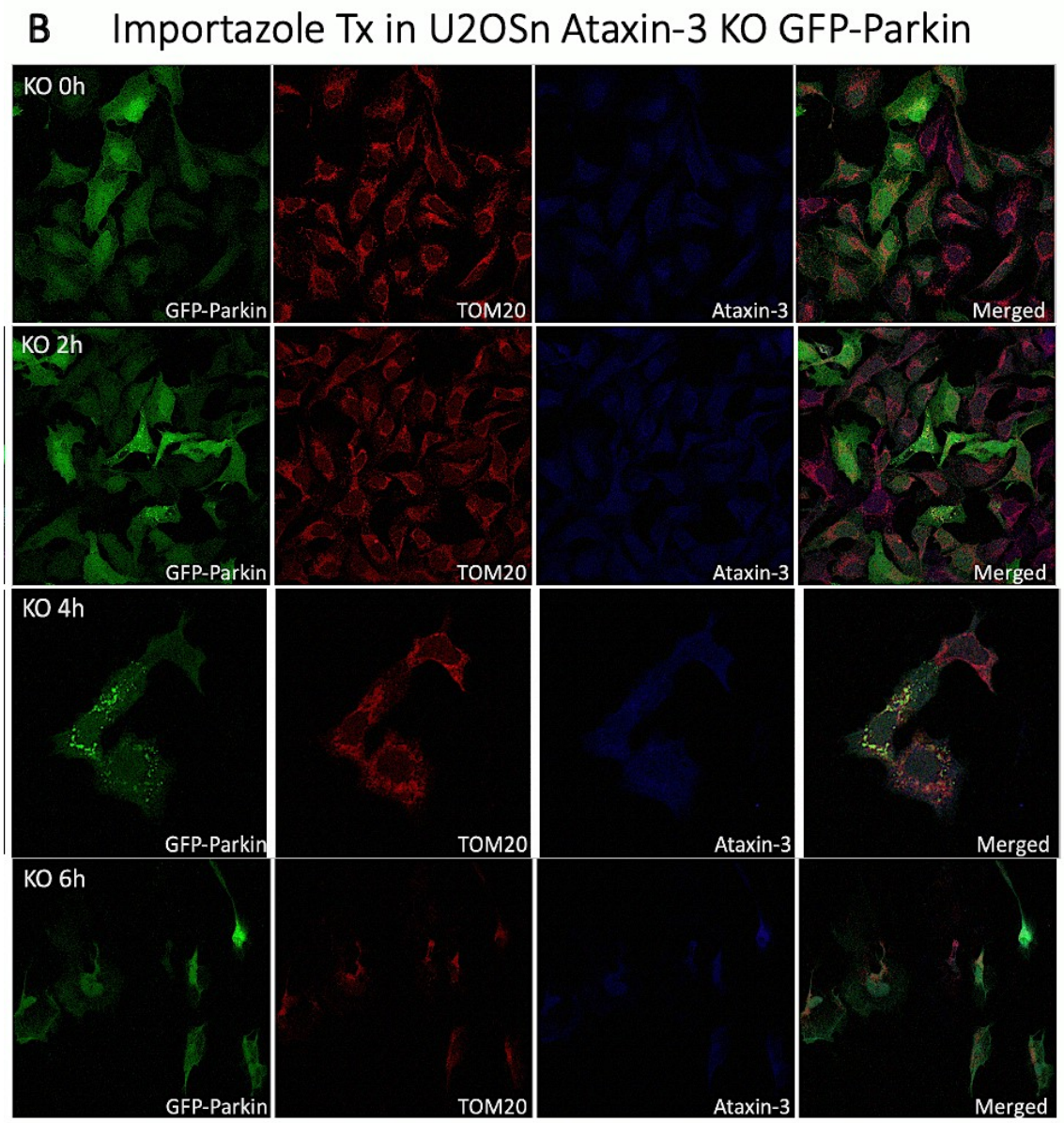

<u>Figure 17.</u> Parkin recruitment using importazole.
Importazole treatment in (**A**) wildtype U2OSn GFP-Parkin and (**B**) U2OSn ataxin-3 KO GFP-Parkin cells showed parkin recruitment at multiple time intervals. However, there was no difference on recruitment between KO and parental line under confocal microscopy.

Measuring parkin recruitment by WB

To observe protein recruitment, as well as to measure the turnover effect of parkin and Mitofusin2 (Mfn2), an outer mitochondrial membrane protein involved in mitochondrial function, U2OSn ataxin-3 KO GFP-parkin cells were treated with 20μM CCCP for 0h, 2h, 4h, and 24h. WB of CCCP treated cells blotted for different proteins showed no difference in turnover of Mfn2 or parkin. As a result, there is no conclusive evidence for differences in parkin or Mfn2 turnover in CCCP treated cells with and without endogenous ataxin-3 (**Figure 18**).

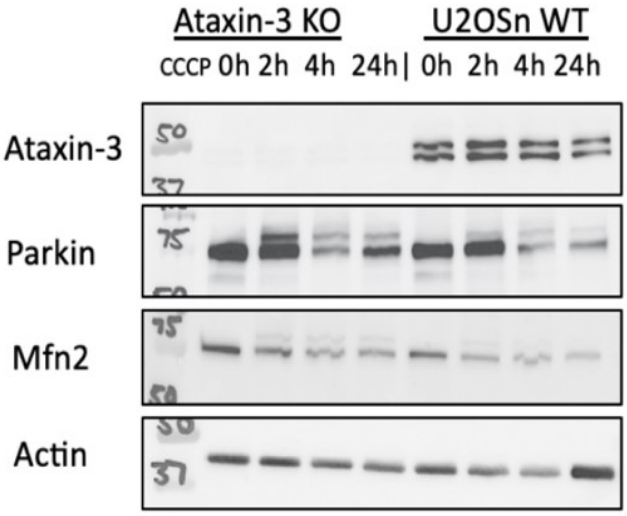

Figure 18. Immunoblot of protein turnover upon CCCP treatment.
WB showing levels of ataxin-3, parkin, and Mfn2 in U2OSn ataxin-3 KO GFP-Parkin cells after CCCP time interval treatments of 0h (control), 2h, 4h, and 24h.

Overall, throughout this research using immunoblotting, live imaging, and confocal microscopy to observe parkin recruitment, turnover, and mitochondrial membrane potential, negligible effects on parkin recruitment and no effect on turnover of mitochondrial proteins were demonstrated in the absence of ataxin-3.

Measuring turnover in ataxin-3 KO cells

Lastly, while the absence of ataxin-3 in cells does not seem to have effect on parkin stability, ataxin-3 KO may affect mitochondrial turnover. Thus, a mt-Keima assay to quantify mitochondria turnover was done on U2OSn ataxin-3 KO GFP-Parkin cells. Mt-Keima is a useful method to determine mitophagy activation in cells [88] since the protein emits different signals with changes in its pH environment indicating mitophagy and degradation, and it was used to determine whether ataxin-3 KO had an effect on parkin function. Transiently transfected U2OSn ataxin-3 GFP-Parkin cells with induced mt-Keima and treated with CCCP to induce mitochondrial depolarization and subsequent mitophagy were analyzed using FACS. Flow cytometry measured the percentage of GFP-Parkin and mt-Keima double-positive cells that are undergoing mitophagy for each sample and are illustrated by the mitophagy percentage. Looking at the results, 2,000 to 8,000 cells were analyzed per cell line and it appears there was less mitophagy occurring in the ataxin-3 KOs compared to the wildtype cells, showing an interesting and robust effect between the KO lines and possibly suggesting that the absence of ataxin-3 has an effect on mitochondrial turnover (**Figure 19**).

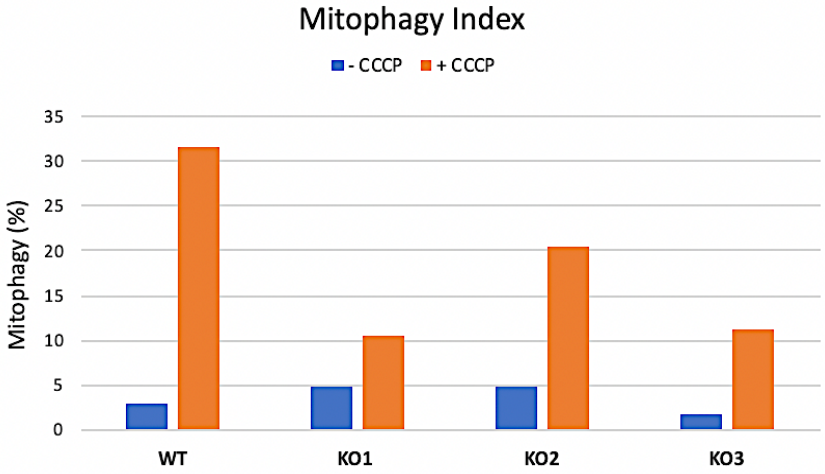

Figure 19. Mt-Keima Assay to Determine Mitochondrial Turnover. Mitophagy index of three U2OSn ataxin-3 KOs GFP-Parkin and the wildtype showing the percentage of double-positive GFP-Parkin and mtKeima cells undergoing mitophagy.

Discussion

SCA3 is a multisystemic neurodegenerative disorder that affects several regions of the brain, such as the cerebellum, midbrain and brainstem, areas mostly involved in movement. To date, there is no effective therapeutic approach that has been developed for SCA3 and other polyQ diseases, and consequently, all remain incurable and fatal. The affected protein of SCA3, ataxin-3, in its polyQ-expanded form is known to aggregate and generate toxic species that disrupt several cell systems including ubiquitination, misfolded protein degradation, transcription, mitochondria quality control, and DNA repair. In its endogenous state, ataxin-3 is implicated in these systems, showing multifunctional roles in the cell.

Since ataxin-3 and parkin are partners in the UPS with opposing roles, and both are involved in neurodegenerative disorders, PD and SCA3, it is known that these disorders have overlapping phenotypes, but the mechanism(s) involved are unknown. In this research, the interest was to see the relationship of parkin function and stability without ataxin-3 present in cells to understand what happens to parkin stability and its function in mitophagy.

To properly validate ataxin-3 KO lines, a characterization process was established to observe ataxin-3 levels using WB and IF applications. For these procedures, the antibody validation process constituted an important step for the course of the project. Antibodies are a fundamental tool in biomedical research, but unfortunately antibody characterization is not on the same quality control as antibody generation and is very problematic for the scientific community. Therefore, it is absolutely essential to have working specific antibodies when doing research. Anti-ataxin-3 antibodies MAB5360 and ProteinTech #13505-1-AP were validated for WB and IF, respectively. Each antibody was authenticated for a different application because their specificity for ataxin-3 differs. MAB5360 is a monoclonal antibody which has specific

binding to a unique epitope, in this case is aa 112-249 on ataxin-3. This high specificity is advantageous for applications such as WB, which aims to quantify protein levels, and indeed resulted in successful recognition of our target protein. On the other hand, ProteinTech #13505-1-AP is a polyclonal antibody which recognizes different epitopes, giving it a high affinity to the antigen and more robust detection. This detection is greater in assays where the native protein is used, such as IF in this research. In the denatured form, we saw cross reactivity and non-specific binding in WB, mostly likely due to ProteinTech #13505-1-AP antibody recognizing these multiple epitopes. These explanations are mostly consistent with what we saw in our screening for antibody validation and explains why each antibody was validated for different applications in this research. Another consideration regarding antibody validation is the location of the KO in ataxin-3. For our CRISPR KO strategy, exon 2 was targeted because the first ATG start was there, and the goal was to create a frameshift and eliminate expression of the translated protein. The Josephin domain lies in exon 2 and observing its location could represent that these cell lines may have an active C-terminal. As far as the literature goes, there are no reported stable cell lines with a Josephin domain KO in ataxin-3. A way to see if our KOs has a mutated Josephin domain is to obtain and screen an ataxin-3 specific C-terminal antibody and blot all our KOs plus parental lines, to then possibly understand if what we have seen throughout the research is because of ataxin-3 deficiency, or a truncated/mutated form of the Josephin domain in ataxin-3.

Once the antibodies were validated using the appropriate validation pipeline [83], clones of the two cell lines of interest where analyzed to identify those with no ataxin-3 expression. Both CRISPR generated HEK293T and U2OSn ataxin-3 KO cell lines demonstrated a homozygous deletion in the KOs via genomic sequencing, and in WB no protein expression was shown in the clones compared to the two ataxin-3 alleles in the wildtype cells.

In conjunction with the ataxin-3 KO in both lines, it was important to observe the health, viability, growth, and cell cycle of these cells and examine any changes in homeostasis. With respect to cell growth and proliferation, the HEK293T wildtype cells seemed to proliferate and spread better than the KOs after 24h and continued with this trend until the end of the 35h interval. This tendency was not confirmed with the U2OSn cell line, as there was no significant difference in proliferation between KOs and wildtype cell lines, and growth consistency curves looked more jagged. Granted, U2OS cells are very flat, and the brightfield contrast was less for HEK293T cells, so it was ironically harder for the CellProfiler™ software mask to properly identify the U2OSn cells. The Columbus™ analysis system was used instead with the same criteria parameters with successful quantifiable analysis. However, globally, the cell lines could show a difference in cell growth when ataxin-3 is absent. Ataxin-3-dependent differences in promotion or inhibition of cell proliferation are seen in testicular cancer literature, where over-expression of ataxin-3 promotes cell proliferation, and ataxin-3 knockdown inhibits proliferation in testicular cancer cell lines TCam-2, I-10 and the normal testis line Hs1 [89]. Cell proliferation has been mainly observed in cells expressing polyQ-expanded ataxin-3, where a substantial decrease of proliferation has been observed. This model is used in order to observe pathogenesis, but more research is needed elucidate to whether ataxin-3 depletion affects cell growth in a cell-type dependent manner, since these results were neither expected nor unexpected for ataxin-3.

To further assess cell proliferation in our HEK293T and U2OSn ataxin-3 KOs, longer imaging analysis should be done, perhaps up to 72 hours, to get a better idea of a consistent cell growth trend between all samples. Also, longer passaged cells versus freshly thawed cells could show a difference in cell growth in this analysis if it is true that absence of ataxin-3 might decrease cell growth over time. For a more precise and quantitative way to measure cell

proliferation, the EdU cell proliferation assay kit (ab219801) would be another good alternative to observe cell growth changes between wildtype and KOs. EdU checks the ratio between total cell surface and nuclei by measuring DNA synthesis and can be analyzed via flow cytometry or fluorescence microscopy. Samples can be stained with validated antibody ProteinTech #13505-1-AP for supplementary evaluation if necessary. Additionally, doing any of these cell proliferation experiments with both glucose and galactose-grown U2OSn ataxin-3 KO cells is another noteworthy approach to measure cell growth and ATP content. Given that our results showed slower parkin recruitment upon mitochondrial depolarization, as seen in **Figure 16**, it may also be possible to see slower cell proliferation on galactose-grown cells. The reduction and amplitude of difference between the KOs versus the wildtype could be something to further explore in these cells.

Overall, the removal of ataxin-3 did not seem to alter the cell cycle behavior of either the HEK293T or U2OSn cell lines as measured using the DNA staining agent PI; KOs and wildtype were mostly in G1 growth phase with steady viability, as expected. These observations are consistent with cell cycle analysis from other studies stating that depletion of ataxin-3 showed no effect on the G1 phase under normal conditions, and PI-positive cells are similar to wildtype [12, 90]. However, when cells are under stress conditions, such as X-ray irradiation, or in the polyQ expanded form, the observations were different. HeLa ataxin-3 KO cells generated from another study entered cell cycle faster and had a moderate decrease of G2/M phase populations and expanded ataxin-3 absorbed PI staining by two-fold compared to wildtype [12, 90], while our ataxin-3 KOs did not show this. Therefore, for these HEK293T and U2OSn ataxin-3 KO cell lines, additional stress conditions, such as heat shock or X-ray irradiation, could be applied and then any differences observed compared to the initial findings of stable and viable KOs.

This is interesting to keep in mind for future studies since the next steps will be to broaden the investigation into the function and stability of cell cycle regulators that are known to interact with ataxin-3, such as checkpoint kinase 1 (Chk1) and tumor protein p53 [11, 12]. In its normal state, ataxin-3 as a DUB removes polyUb chains of Chk1 and p53 and regulates their activity to delay cell cycle progression and promote DNA repair, checkpoint signaling and cell survival. Ataxin-3 deletion in MEFs reduced p53 protein levels and inhibited its transactivation activity [11]. For Chk1, MEF ataxin-3 KOs had elevated turnover, were less stable, and therefore had impaired DNA damage checkpoints [12]. So, without ataxin-3 as a DUB in the model cell lines generated during this project, it will be important to test the general genome integrity and cell homeostasis to understand if these same regulators and their mechanisms are compromised, and if any additional pathways could be affected.

For example, when looking at parkin recruitment, importazole unexpectedly impaired cell viability in the ataxin-3 KO cells (**Figure 17**). When doing all three independent IF experiments, almost all ataxin-3 KO cells were dead after incubation with importazole for 4h and onwards. Wildtype cells were affected as well, but it was mostly the KOs which had complete cell death. These unexpected findings relate to findings where scientists were studying the effect of importazole on cell cycle and apoptosis in myeloma cells, and discovered that importazole inhibited cell proliferation, reduced DNA binding activity and induced apoptosis in these cells by obstructing the NF-κB signaling pathway *in vitro* [91]. NF-κB is a protein complex that when activated, it controls DNA transcription and cell survival [92, 93]. Since NF-κB activation is involved in survival, it is tightly regulated by the UPS. NF-κB is inhibited in the cytoplasm by IκB proteins, and when activated, the IκBα protein is phosphorylated, polyubiquitinated, and ultimately degraded by the 26S proteasome; NF-κB then dissociates from the complex and enters

the nucleus to regulate its target genes [94]. It has been shown that parkin, aside from its role in mitophagy, is involved in this pro-survival signaling pathway and prevents mitochondrial impairment and promotes survival by increasing ubiquitination of NF-κB essential modulator (NEMO) and upregulating NF-κB target genes such as OPA1, a gene that helps regulate mitochondria integrity and fusion [95, 96]. Additionally, valosin containing protein (VCP/p97), a protein involved in extracting proteins from the ERAD, is involved in activating complex NF-κB, as well as chaperoning the polyUb IκBa to the 26S proteasome for degradation [94]. VCP/p97 and ataxin-3 have been shown to bind and be involved in the retrotranslocation of ubiquitinated substrates from the endoplasmic reticulum in the ERAD, as ataxin-3 binds to VCP/p97 and decreases the extraction of these ERAD substrates [97, 98], and VCP/p97 enhances the enzymatic activity of endogenous ataxin-3 [99]. Moreover, studies have confirmed a relationship exists with polyQ expanded ataxin-3 to the NF-κB signaling pathway. In drosophila SCA3 models, increasing NF-κB activation reduced reactive oxygen species and autophagy of cells with mutant ataxin-3 [100]. In the expanded form, IκB proteins have been shown to have increased accumulation and associate with polyQ expanded ataxin-3 and huntingtin protein in wildtype mouse Neuro-2a and COS-1 cells. Additionally, polyQ expanded ataxin-3 downregulates NF-κB activity, possibly leading to neurodegeneration and expanded polyQ protein-induced cell death [101]. It is possible that a connection exists between ataxin-3, parkin, VCP/p97 and the NF-κB complex and this may be worth examining. There is little to no research on the NF-κB pathway in the presence or absence of endogenous ataxin-3. Thus, further understanding of ataxin-3 and the NF-κB signal pathway could be of interest when investigating ataxin-3 and its effect on transcription, proliferation, and DNA binding, and if the removal of ataxin-3 has any implications. More research should be done with importazole on ataxin-3 since this connection

most likely affects the UPS, ERAD and may have a link to mechanisms involved in cell survival, thus this dynamic interaction might have a role in the pathogenesis of SCA3.

Mitochondria are the powerhouse of the cell, and mitochondrial dysfunction has been seen in many neurodegenerative diseases; SCA3 is not an exception. Toxic fragments of expanded ataxin-3 cause problems throughout the cell, including in the mitochondria [68, 69]. In our studies, ataxin-3 KO cells were used to measure several mitochondrial functions. First, there were no changes in the protein levels of outer membrane proteins, such as Mfn2, in ataxin-3 KO cells. This shows that the mitochondrial network is still maintained without the need for the presence of ataxin-3. Second, upon CCCP treatment, U2OSn ataxin-3 KO GFP-Parkin cells grown in galactose DMEM had slower mitochondrial translocation of parkin compared to glucose-grown cells, as observed previously [66]; and both cell lines regardless of DMEM showed co-localization of parkin with the mitochondria, but there was no difference in parkin recruitment compared to the wildtype. This reveals that ataxin-3 has no impact on parkin recruitment and function in these cell lines. Lastly, looking at mitochondrial membrane potential, high glycolytic cells had no difference in TMRM intensity compared to cells grown in galactose, as expected, but galactose-grown cells showed decreased potential in the wildtype compared to ataxin-3 KO. Since cells cultured in galactose are more vulnerable to mitochondrial stressors as they don't receive the substrate that allow the ATP production through glycolysis, and this implies that cells are more active in glucose-grown media as it’s driving additional ATP production. For galactose-grown cells with an increased potential in the KOs, this could mean that the ETC is working faster and leading to increased ATP production. Or perhaps when ataxin-3 is absent, there is no recognition of oxidative stress, causing an increase in the potential.

Future directions on mitochondrial respiration in ataxin-3 KO cells could involve a Seahorse assay in order to measure both energy pathways of the cell (mitochondrial respiration and glycolysis). This assay would measure the rate of oxygen consumption in the galactose-grown cells and the lactic acid production of the glycolytic cells to compare the extracellular flux of both cell lines in real time. This way it could compliment the TMRM results and help determine the bioenergetic status of the cells lacking functional ataxin-3.

To explore the parkin-ataxin-3 relationship, parkin stability was measured in ataxin-3 KO cells and compared to wildtype cells. Overall, WB and quantitative LI-COR analysis revealed there were no alterations in relative levels of parkin in ataxin-3-depleted cell lines, which was anticipated and also observed before in mice models[8] , showing a normal cellular expression for parkin even when ataxin-3 is not there. The normal function of parkin in these cell lines is important because it demonstrates that ataxin-3 is not really required for parkin to function normally. Collectively, ataxin-3 levels were measured in HEK293T parkin KO cell lines, and consistently there was no effect on ataxin-3 protein levels. Even under stressed conditions with CCCP treatment, parkin recruitment did not seem to change in wildtype versus ataxin-3 KO. This suggests parkin carries out its roles, such as recruitment, in a normal manner without being affected by the absence of ataxin-3.

While it does not appear to have an effect on parkin stability, the absence of ataxin-3 might possibly have an effect on mitochondrial turnover. Our last aim was to do a mt-Keima assay to quantify mitochondria turnover in U2OSn ataxin-3 KO GFP-Parkin cells. Transiently transfecting cells with the mt-Keima protein showed there is surprisingly less mitophagy occurring in the KOs compared to the wildtype, possibly meaning that ataxin-3 may have an effect of mitochondrial turnover. This is a key finding for this research. Unfortunately, due to

COVID-19 and subsequent lab shutdown in March 2020, the mt-Keima assay was only done once so there is no available statistics and no additional replicated experiments done, but the effect on this one time experiment seems encouraging, as all KO lines showed less mitophagy than the wildtype when treated with CCCP. For the mt-Keima assay to be more robust, a stable line of mt-Keima protein-expressing U2OSn ataxin-3 KO GFP-Parkin cells will be better than the transiently transfected cells. This is because the number of double-positive GFP-parkin + keima cells was low in our assay, and a higher number of cells with mitophagy percentage events will determine if mitophagy is indeed reduced in the KOs. Additionally, replicating this experiment with overexpression of ataxin-3 would be important in order to see if we get the opposite effect of turnover from wildtype and expanded polyQ form. Mt-Keima assay on galactose-grown U2OSn ataxin-3 GFP-Parkin cells is also an attractive way to compare mitochondrial turnover and metabolism with glucose-grown U2OSn ataxin-3 KO GFP-Parkin cells.

From all these findings, a model figure (**Figure 20**) incorporating these results helped to visualize how the absence of ataxin-3 might impact on normal functions within the cell in order to fully understand the complex picture of ataxin-3 function.

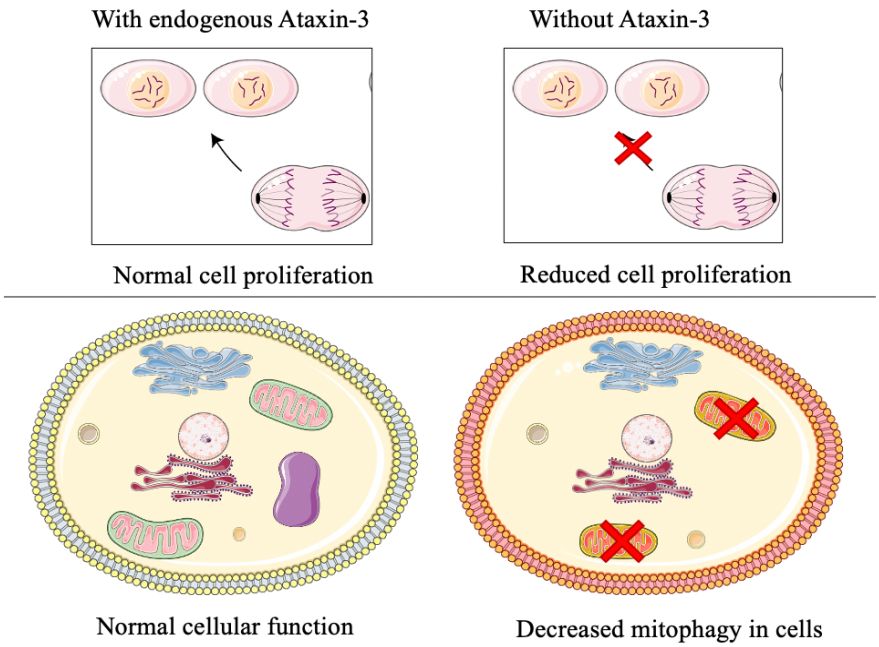

Figure 20. Potential impact of ataxin-3 on the normal cell function.
In the cell, when endogenous ataxin-3 is present, the organelles seem to do their roles and functions normally, as well as the function of cell division growth.
The absence of ataxin-3 might have a possible effect on cell proliferation and an effect on mitochondrial turnover, the crosses depict these alterations when the ataxin-3 protein (in purple) is no longer there.

Based on what we saw with the mt-Keima assay, if ataxin-3 is involved in the mitophagy pathway, it could be downstream of parkin, since it deubiquitinates parkin. So perhaps the deubiquitination of parkin is necessary for a more robust mitophagy response, and if parkin remains ubiquitinated it gets turned over faster and can't potentiate the response on the mitochondria. Correspondingly, Beclin 1, a component that initiates autophagy, interacts with the polyQ tract of ataxin-3 and protects Beclin 1 from degradation [102]. With expanded polyQ ataxin-3, it binds to Beclin 1 to a greater extent and promotes its degradation. This might explain how the mutant polyQ tract can impair autophagy formation and initiation, and therefore reduce mitophagy initiation as well. Decreased levels of Beclin 1 have been seen in SCA3, HD, and

Alzheimer's Disease [103-105]. Subsequently, due to the absence of ataxin-3 in the KO cells, if ataxin-3 is not there to bind to and stabilize Beclin 1, this could also explain the reduced mitophagy in the KO cells. Additionally, Beclin 1 is involved in translocating parkin to mitochondria as well as parkin-induced mitophagy [102]. The mechanisms of how the binding and interaction of these proteins play out are yet to be defined to clarify the role of ataxin-3 in mitochondrial quality control. Mitochondria are dynamic organelles that move and continually undergo fission and fusion events in response to the demands of the cell and the morphology of mitochondria is directly linked to the maintenance of mitochondrial functions [106, 107]. For that reason, investigating mitochondrial morphology, size, and shape in ataxin-3-depleted cells could be a subsequent focus when looking at mitochondria stability. It has been widely researched using the mutated form of ataxin-3, showing aberrant morphology and irregular metabolism in cells and mouse models [68, 69, 71, 73], but the loss of ataxin-3 in mitochondrial function has not been extensively investigated.

The UPS has also been associated with regulating mitochondrial function as a part of its overall quality control system. Several studies have demonstrated that the UPS participates in recycling mitochondrial-associated proteins, initially from proteomic screens of mitochondria that have classified more than 100 proteins that can undergo ubiquitination and are targeted to the UPS for degradation [108-110]. The proteins identified in the screen are associated with multiple mitochondrial functions that include ATP production through oxidative phosphorylation and biosynthesis of fatty acids [108]. The proteasome is responsible for the degradation of proteins at the mitochondria, more specifically proteins on the outer mitochondrial membrane (OMM) that share an interface with the cytoplasm. Some widely studied examples of OMM proteins that are degraded in a proteasome-dependent manner include Mcl-1, a pro survival member of the Bcl-2

family [111]; Drp1, a mitochondrial fission protein and substrate of parkin [112]; Mfn1 and Mfn2, regulators of mitochondrial fusion [113]. These findings underline the influence the UPS has in regulating mitochondrial membrane dynamics.

There are several stages within mitochondrial quality control pathways where DUBs can intersect. For instance, DUBs may oversee the activity of mitochondrial E3s and consequently regulate protein quality control via the proteasome. Alternatively, DUBs can regulate the formation of Ub conjugates on mitochondrial substrates, thereby influencing the turnover of substrates. From previous studies, there are four known mitochondria-associated DUBs. These include USP8, USP15, USP30, USP36, USP9x and ataxin-3 [65, 109, 114]. USP8 is a DUB required for parkin recruitment to the mitochondria, and it directly deubiquitinates parkin by preferentially removing K6-linkage chains within parkin-Ub conjugates [115]. USP15 is predominantly cytosolic but also partially colocalized in the mitochondria, and it counteracts parkin-mediated accumulation of K48 and K63-linked chains on mitochondrial substrates, such as Mfn2 [116]. USP30 is a mitochondrial-anchored DUB that resides in the OMM and specifically cleaves parkin generated K11-, K63-, and preferred K6-linked Ub chains on mitochondrial substrates and thereby inhibiting mitophagy [117, 118]. USP36 is localized in the nucleoli of the mitochondria and regulates its nucleolar activity [109]. USP9x is involved in neuronal fate by cleaving K48 chains of Mc1-1 in the OMM. Last but not least, Ataxin-3 has the ability to cleave to a variety of Ub chain types, including K6, K27, K29, K48, and K63, yet it has a preference to cleave K63 in particular [8, 109]. Additionally, out of these DUBs, USP8, USP15, ataxin-3 and USP30 have been found to have a role in modulating parkin auto-ubiquitination and parkin-mediated mitophagy [65], where USP8 deubiquitinates parkin directly, ataxin-3 is able to counteract the several types of parkin Ub conjugations, and both USP15 and USP30 act as a regulators of mitophagy by counteracting the ubiquitination of mitochondrial substrates [119].

Precisely, a DUB to keep in mind when it comes to the connection between mitochondrial quality control, ataxin-3, and parkin is USP30. This mitochondrial deubiquitinase inhibits mitophagy by removing Ub conjugates from Mfn2, TOM20, TOM70 and mitochondrial porins, and therefore mitochondria is no longer directed to the proteasome [65, 117]. On the other hand, knockdown of USP30 increases fission activities thus changing mitochondrial morphology [120], and increasing turnover as K48 chains form on substrates at a higher level [65, 108, 117]. Overall, these observations link USP30 in several important mitochondrial directed activities. Additional to USP30, mitophagy is also kept in check by other DUBs, such as USP8, USP15 and USP35, which also remove ubiquitin tags acting as a "stop sign" for the pathway. But this is not the case for ataxin-3. Ataxin-3 is not a DUB that acts directly on mitophagy, instead it is a modulator of parkin that likely edits Ub chains to target parkin to different cellular pathways, such as DNA repair and autophagy. Parkin, once activated, forms different polyUb chains and ubiquitinates many substrates with K48- and K63-linked ubiquitin chains, as well as K6, K11, K27 chains [65]. K63-linked chains are proposed to act as the Ub label for autophagy and are recognized by different autophagy receptors, and K48-linked chains have been suggested to be the principal signal for UPS degradation [121, 122]. K6 linkages are primarily involved in parkin-mediated mitophagy as well as DNA repair [65], while K11 and K27 elaborate on cell cycle and nuclear translocation [123, 124]. Therefore, when ataxin-3 is not there, parkin is free to form any chains it wants. Based on the results of the mt-Keima assay, this might imply that parkin forms excess K6 chains that impede turnover in the KOs.

Therefore, a next step for this project is to make a double KO cell line removing USP30 in the ataxin-3 KO background. In the absence of USP30, there will be enhanced turnover of mitochondrial substrates due to increased levels of K48 chains, and without

ataxin-3, parkin will be free to form other chains, so it will shift from making K48-linked chains to K6 chains, which in theory might mitigate the effect of USP30 removal and consequently balancing mitophagy. Since USP8 directly deubiquitinates parkin by hydrolyzing K6 chains, it is something to keep in mind when seeing effect of USP30 removal in ataxin-3 KO cell line. Thus, further investigation and *in vitro* work must be done in order to confirm this hypothesis to first have baseline effects and then measure how this can go on into a neuronal context.

There are several directions in which this research project could evolve for a more future approach. A potential role to establish in the long-term is the effect of ataxin-3 KO in a neuronal cell line, and in particular within cerebellar organoids. Since both ataxin-3 and parkin are abundant in neurons, it is only appropriate to advance this research in *in vitro* culture systems to test these questions within a neuronal system, and not just within several more immortalized cell-lines. This research could also be worthwhile to translate into a more dynamic approach, where a KO of ataxin-3 is implemented in human induced pluripotent stem cells (iPSCs) in order to model and further reveal its role in a unique human context unmatched by mouse models or cell lines. An intriguing idea is to make an iPSC line with both ataxin-3 and parkin KO, or an ataxin-3 and USP30 KO, and further understand the mechanism of their relationship, by looking at the UPS pathway as well as mitophagy. At present, most iPSC cell lines have been generated with the mutated form [125, 126] or removing the polyQ encoded region of ataxin-3 [127], but no studies have knocked out the *ATXN3* gene itself. This pioneering work for SCA3 will broaden the research on the functional role of ataxin-3 in the mitochondrial quality control pathway with parkin and elaborate on the physiological function of ataxin-3. It is anticipated that the future

directions proposed in this discussion will tackle and clarify some of the questions posed throughout this thesis based on the results of the work completed.

Conclusion

All ten neurodegenerative polyQ diseases involve proteins of different functions that only contain the polyQ tract in similarity, and it is the genetic mutation in this region that causes each independent polyQ disease. Multiple characteristics of the pathogenesis of these diseases have been investigated throughout several decades, such as protein misfolding and aggregation, nuclear inclusions, transcriptional dysfunction, autophagy, subcellular localization, cellular homeostasis, mitochondrial deregulation, and protein quality control with both the expanded and normal forms of each protein. The work presented in this thesis specifically examined the role of ataxin-3, the protein of interest involved in SCA3, in cellular homeostasis, mitochondrial quality control and protein stability. Studying cellular and mitochondrial quality control along with function and protein interactions in the presence and absence of ataxin-3 in cells has been important in the understanding parkin-ataxin-3 relationship, particularly in mitochondrial turnover. This project set out to determine if ataxin-3 removal had any effect on parkin stability and function in the cell and in the mitochondrial system using validated KO tools created and characterized as described within this thesis.

In conclusion, this thesis data has demonstrated that removal of ataxin-3 had no overt effect in the cycling behavior of cells when using PI staining, no alterations in parkin levels or stability in ataxin-3 KO cell lines using WB and LI-COR analysis, no significant difference in mitochondrial membrane potential in the TMRM experiment, and there was a maintained mitochondrial network without the presence of ataxin-3 and no changes in levels of outer membrane proteins, such as Mfn2 in KO cells. However, this researched has successfully

showed that there was an alteration in cell proliferation in HEK293T ataxin-3 KO cells compared to wildtype, and although there were no differences in parkin recruitment between wildtype and ataxin-3 KO lines using CCCP and importazole treatment, there were treatment-dependent differences in the distribution of GFP-Parkin. Additionally, for importazole, there was greater cell death observed in U2OSn ataxin-3 KO GFP-Parkin cells when treated with importazole compared to wildtype. Most importantly, there was a turnover effect in ataxin-3 KO cells from the Mt-Keima assay, suggesting ataxin-3 has a possible role on the mitophagy pathway and related proteins.

Because of these results, this project opened up several interesting questions worth exploring, specifically the effect of cell proliferation in ataxin-3 depleted cells, a decreased mitophagy turnover effect in the KOs, and a further connection of ataxin-3 with several DUBS in parkin-mediated mitochondrial degradation. We now have validated tools: effective ataxin-3 KO cell lines and validated antibodies to use for future research on the role of ataxin-3 and elucidate then how the expanded polyQ ataxin-3 plays a role in the pathogenesis of SCA3.

Given that parkin is an E3 ligase involved in the UPS as well as mitochondrial degradation, and ataxin-3 is a DUB in the UPS with potential influence on the mitophagy pathway, the mechanistic understanding of the interplay between these two cellular systems is still needed to be investigated and clarified. Hence, further studies are required to investigate mitochondrial UPS, the mitophagy pathway, and the several proteins involved in the mutual interplay between these two processes to understand how dysfunction of these systems relate to overall cellular metabolic states. New discoveries in these mitochondrial quality control systems and their functions in global cell integrity will continue to enlighten scientists on the pathogenesis of neurodegenerative diseases like SCA3 and PD. Creating a KO to abolish ataxin-3 expression

helped elucidate what effect its absence might have on distinct molecular cellular processes. These investigations have shown how a loss in functional ataxin-3 could impact specific pathways, including the cell cycle, mitochondrial quality control and the interconnection of the UPS. These results could effectively explain the cellular function of ataxin-3, parkin and other proteins and potentially enhance our understanding on the role ataxin-3 has in the cell and how this might be linked to the neurodegenerative features of SCA3.

References

1. Maciel, P., et al., *Correlation between CAG repeat length and clinical features in Machado-Joseph disease.* Am J Hum Genet, 1995. **57**(1): p. 54-61.
2. Da Silva, J.D., A. Teixeira-Castro, and P. Maciel, *From Pathogenesis to Novel Therapeutics for Spinocerebellar Ataxia Type 3: Evading Potholes on the Way to Translation.* Neurotherapeutics, 2019. **16**(4): p. 1009-1031.
3. McLoughlin, H.S., L.R. Moore, and H.L. Paulson, *Pathogenesis of SCA3 and implications for other polyglutamine diseases.* Neurobiol Dis, 2020. **134**: p. 104635.
4. Rub, U., et al., *Clinical features, neurogenetics and neuropathology of the polyglutamine spinocerebellar ataxias type 1, 2, 3, 6 and 7.* Prog Neurobiol, 2013. **104**: p. 38-66.
5. Scherzed, W., et al., *Pathoanatomy of cerebellar degeneration in spinocerebellar ataxia type 2 (SCA2) and type 3 (SCA3).* Cerebellum, 2012. **11**(3): p. 749-60.
6. Seidel, K., et al., *Brain pathology of spinocerebellar ataxias.* Acta Neuropathol, 2012. **124**(1): p. 1-21.
7. Paulson, H.L., et al., *Intranuclear inclusions of expanded polyglutamine protein in spinocerebellar ataxia type 3.* Neuron, 1997. **19**(2): p. 333-44.
8. Durcan, T.M., et al., *The Machado-Joseph disease-associated mutant form of ataxin-3 regulates parkin ubiquitination and stability.* Hum Mol Genet, 2011. **20**(1): p. 141-54.
9. Burnett, B., F. Li, and R.N. Pittman, *The polyglutamine neurodegenerative protein ataxin-3 binds polyubiquitylated proteins and has ubiquitin protease activity.* Hum Mol Genet, 2003. **12**(23): p. 3195-205.
10. Li, F., et al., *Ataxin-3 is a histone-binding protein with two independent transcriptional corepressor activities.* J Biol Chem, 2002. **277**(47): p. 45004-12.
11. Liu, H., et al., *The Machado-Joseph Disease Deubiquitinase Ataxin-3 Regulates the Stability and Apoptotic Function of p53.* PLoS Biol, 2016. **14**(11): p. e2000733.
12. Tu, Y., et al., *Ataxin-3 promotes genome integrity by stabilizing Chk1.* Nucleic Acids Res, 2017. **45**(8): p. 4532-4549.
13. Zeng, L., et al., *Loss of the Spinocerebellar Ataxia type 3 disease protein ATXN3 alters transcription of multiple signal transduction pathways.* PLoS One, 2018. **13**(9): p. e0204438.
14. Kitada, T., et al., *Mutations in the parkin gene cause autosomal recessive juvenile parkinsonism.* Nature, 1998. **392**(6676): p. 605-8.
15. Coutinho, P. and C. Andrade, *Autosomal dominant system degeneration in Portuguese families of the Azores Islands. A new genetic disorder involving cerebellar, pyramidal, extrapyramidal and spinal cord motor functions.* Neurology, 1978. **28**(7): p. 703-9.
16. Healton, E.B., et al., *Presumably Azorean disease in a presumably non-Portuguese family.* Neurology, 1980. **30**(10): p. 1084-9.
17. Lima, L. and P. Coutinho, *Clinical criteria for diagnosis of Machado-Joseph disease: report of a non-Azorena Portuguese family.* Neurology, 1980. **30**(3): p. 319-22.
18. Gispert, S., et al., *Chromosomal assignment of the second locus for autosomal dominant cerebellar ataxia (SCA2) to chromosome 12q23-24.1.* Nat Genet, 1993. **4**(3): p. 295-9.
19. Takiyama, Y., et al., *The gene for Machado-Joseph disease maps to human chromosome 14q.* Nat Genet, 1993. **4**(3): p. 300-4.
20. Den Dunnen, W.F.A., *Trinucleotide repeat disorders.* Handb Clin Neurol, 2017. **145**: p. 383-391.

21. Cummings, C.J. and H.Y. Zoghbi, *Trinucleotide repeats: mechanisms and pathophysiology.* Annu Rev Genomics Hum Genet, 2000. **1**: p. 281-328.
22. Zhou, J., et al., *Functional classification and mutation analysis of a synpolydactyly kindred.* Exp Ther Med, 2014. **8**(5): p. 1569-1574.
23. Albrecht, A. and S. Mundlos, *The other trinucleotide repeat: polyalanine expansion disorders.* Curr Opin Genet Dev, 2005. **15**(3): p. 285-93.
24. Adegbuyiro, A., et al., *Proteins Containing Expanded Polyglutamine Tracts and Neurodegenerative Disease.* Biochemistry, 2017. **56**(9): p. 1199-1217.
25. Lieto, M., et al., *The complex phenotype of spinocerebellar ataxia type 48 in eight unrelated Italian families.* Eur J Neurol, 2020. **27**(3): p. 498-505.
26. Sullivan, R., et al., *Spinocerebellar ataxia: an update.* J Neurol, 2019. **266**(2): p. 533-544.
27. Sudarsky, L. and P. Coutinho, *Machado-Joseph disease.* Clin Neurosci, 1995. **3**(1): p. 17-22.
28. Taroni, F. and S. DiDonato, *Pathways to motor incoordination: the inherited ataxias.* Nat Rev Neurosci, 2004. **5**(8): p. 641-55.
29. Durr, A., *Autosomal dominant cerebellar ataxias: polyglutamine expansions and beyond.* Lancet Neurol, 2010. **9**(9): p. 885-94.
30. Paulson, H.L., et al., *Polyglutamine spinocerebellar ataxias - from genes to potential treatments.* Nat Rev Neurosci, 2017. **18**(10): p. 613-626.
31. Gardiner, S.L., et al., *Prevalence of Carriers of Intermediate and Pathological Polyglutamine Disease-Associated Alleles Among Large Population-Based Cohorts.* JAMA Neurol, 2019. **76**(6): p. 650-656.
32. Kraft, S., et al., *Adult onset spinocerebellar ataxia in a Canadian movement disorders clinic.* Can J Neurol Sci, 2005. **32**(4): p. 450-8.
33. Storey, E., et al., *Frequency of spinocerebellar ataxia types 1, 2, 3, 6, and 7 in Australian patients with spinocerebellar ataxia.* Am J Med Genet, 2000. **95**(4): p. 351-7.
34. Vale, J., et al., *Autosomal dominant cerebellar ataxia: frequency analysis and clinical characterization of 45 families from Portugal.* Eur J Neurol, 2010. **17**(1): p. 124-8.
35. Soong, B.W., et al., *Frequency analysis of autosomal dominant cerebellar ataxias in Taiwanese patients and clinical and molecular characterization of spinocerebellar ataxia type 6.* Arch Neurol, 2001. **58**(7): p. 1105-9.
36. Alonso, E., et al., *Distinct distribution of autosomal dominant spinocerebellar ataxia in the Mexican population.* Mov Disord, 2007. **22**(7): p. 1050-3.
37. Matos, C.A., S. de Macedo-Ribeiro, and A.L. Carvalho, *Polyglutamine diseases: the special case of ataxin-3 and Machado-Joseph disease.* Prog Neurobiol, 2011. **95**(1): p. 26-48.
38. Evert, B.O., et al., *Neuronal intranuclear inclusions, dysregulation of cytokine expression and cell death in spinocerebellar ataxia type 3.* Clin Neuropathol, 2006. **25**(6): p. 272-81.
39. Seidel, K., et al., *On the distribution of intranuclear and cytoplasmic aggregates in the brainstem of patients with spinocerebellar ataxia type 2 and 3.* Brain Pathol, 2017. **27**(3): p. 345-355.
40. Bettencourt, C. and M. Lima, *Machado-Joseph Disease: from first descriptions to new perspectives.* Orphanet J Rare Dis, 2011. **6**: p. 35.
41. Moro, A., et al., *Spinocerebellar ataxia type 3: subphenotypes in a cohort of Brazilian patients.* Arq Neuropsiquiatr, 2014. **72**(9): p. 659-62.

42. Gwinn-Hardy, K., et al., *Spinocerebellar ataxia type 3 phenotypically resembling parkinson disease in a black family.* Arch Neurol, 2001. **58**(2): p. 296-9.
43. Klinke, I., et al., *Neuropsychological features of patients with spinocerebellar ataxia (SCA) types 1, 2, 3, and 6.* Cerebellum, 2010. **9**(3): p. 433-42.
44. Park, H., H.J. Kim, and B.S. Jeon, *Parkinsonism in spinocerebellar ataxia.* Biomed Res Int, 2015. **2015**: p. 125273.
45. Whaley, N.R., S. Fujioka, and Z.K. Wszolek, *Autosomal dominant cerebellar ataxia type I: a review of the phenotypic and genotypic characteristics.* Orphanet J Rare Dis, 2011. **6**: p. 33.
46. Mendonca, L.S., et al., *Stem Cell-Based Therapies for Polyglutamine Diseases.* Adv Exp Med Biol, 2018. **1049**: p. 439-466.
47. Matos, C.A., L.P. de Almeida, and C. Nobrega, *Machado-Joseph disease/spinocerebellar ataxia type 3: lessons from disease pathogenesis and clues into therapy.* J Neurochem, 2019. **148**(1): p. 8-28.
48. Diallo, A., et al., *Survival in patients with spinocerebellar ataxia types 1, 2, 3, and 6 (EUROSCA): a longitudinal cohort study.* Lancet Neurol, 2018. **17**(4): p. 327-334.
49. Wang, G., et al., *Machado-Joseph disease gene product identified in lymphocytes and brain.* Biochem Biophys Res Commun, 1997. **233**(2): p. 476-9.
50. Trottier, Y., et al., *Heterogeneous intracellular localization and expression of ataxin-3.* Neurobiol Dis, 1998. **5**(5): p. 335-47.
51. Gaspar, C., et al., *Ancestral origins of the Machado-Joseph disease mutation: a worldwide haplotype study.* Am J Hum Genet, 2001. **68**(2): p. 523-8.
52. Carvalho, D.R., et al., *Homozygosity enhances severity in spinocerebellar ataxia type 3.* Pediatr Neurol, 2008. **38**(4): p. 296-9.
53. Macedo-Ribeiro, S., et al., *Nucleocytoplasmic shuttling activity of ataxin-3.* PLoS One, 2009. **4**(6): p. e5834.
54. Breuer, P., et al., *Nuclear aggregation of polyglutamine-expanded ataxin-3: fragments escape the cytoplasmic quality control.* J Biol Chem, 2010. **285**(9): p. 6532-7.
55. Busch, H., *Ubiquitination of proteins.* Methods Enzymol, 1984. **106**: p. 238-62.
56. Costa Mdo, C. and H.L. Paulson, *Toward understanding Machado-Joseph disease.* Prog Neurobiol, 2012. **97**(2): p. 239-57.
57. Harris, G.M., et al., *Splice isoforms of the polyglutamine disease protein ataxin-3 exhibit similar enzymatic yet different aggregation properties.* PLoS One, 2010. **5**(10): p. e13695.
58. Durcan, T.M. and E.A. Fon, *Mutant ataxin-3 promotes the autophagic degradation of parkin.* Autophagy, 2011. **7**(2): p. 233-4.
59. Scaglione, K.M., et al., *Ube2w and ataxin-3 coordinately regulate the ubiquitin ligase CHIP.* Mol Cell, 2011. **43**(4): p. 599-612.
60. Ying, Z., et al., *Gp78, an ER associated E3, promotes SOD1 and ataxin-3 degradation.* Hum Mol Genet, 2009. **18**(22): p. 4268-81.
61. Pfeiffer, A., et al., *Ataxin-3 consolidates the MDC1-dependent DNA double-strand break response by counteracting the SUMO-targeted ubiquitin ligase RNF4.* EMBO J, 2017. **36**(8): p. 1066-1083.
62. Durcan, T.M., et al., *Ataxin-3 deubiquitination is coupled to Parkin ubiquitination via E2 ubiquitin-conjugating enzyme.* J Biol Chem, 2012. **287**(1): p. 531-41.

63. Seirafi, M., G. Kozlov, and K. Gehring, *Parkin structure and function.* FEBS J, 2015. **282**(11): p. 2076-88.
64. Trempe, J.F., et al., *Structure of parkin reveals mechanisms for ubiquitin ligase activation.* Science, 2013. **340**(6139): p. 1451-5.
65. Durcan, T.M. and E.A. Fon, *The three 'P's of mitophagy: PARKIN, PINK1, and post-translational modifications.* Genes Dev, 2015. **29**(10): p. 989-99.
66. McLelland, G.L., et al., *Mfn2 ubiquitination by PINK1/parkin gates the p97-dependent release of ER from mitochondria to drive mitophagy.* Elife, 2018. **7**.
67. McLelland, G.L., et al., *Parkin and PINK1 function in a vesicular trafficking pathway regulating mitochondrial quality control.* EMBO J, 2014. **33**(4): p. 282-95.
68. Harmuth, T., et al., *Mitochondrial Morphology, Function and Homeostasis Are Impaired by Expression of an N-terminal Calpain Cleavage Fragment of Ataxin-3.* Front Mol Neurosci, 2018. **11**: p. 368.
69. Hsu, J.Y., et al., *The Truncated C-terminal Fragment of Mutant ATXN3 Disrupts Mitochondria Dynamics in Spinocerebellar Ataxia Type 3 Models.* Front Mol Neurosci, 2017. **10**: p. 196.
70. Kazachkova, N., et al., *Patterns of mitochondrial DNA damage in blood and brain tissues of a transgenic mouse model of Machado-Joseph disease.* Neurodegener Dis, 2013. **11**(4): p. 206-14.
71. Liu, C.S., et al., *Depletion of mitochondrial DNA in leukocytes of patients with poly-Q diseases.* J Neurol Sci, 2008. **264**(1-2): p. 18-21.
72. Ramos, A., et al., *Differential mtDNA damage patterns in a transgenic mouse model of Machado-Joseph disease (MJD/SCA3).* J Mol Neurosci, 2015. **55**(2): p. 449-53.
73. Yu, Y.C., et al., *Decreased antioxidant enzyme activity and increased mitochondrial DNA damage in cellular models of Machado-Joseph disease.* J Neurosci Res, 2009. **87**(8): p. 1884-91.
74. Weber, J.J., et al., *A combinatorial approach to identify calpain cleavage sites in the Machado-Joseph disease protein ataxin-3.* Brain, 2017. **140**(5): p. 1280-1299.
75. Kristensen, L.V., et al., *Mass spectrometry analyses of normal and polyglutamine expanded ataxin-3 reveal novel interaction partners involved in mitochondrial function.* Neurochem Int, 2018. **112**: p. 5-17.
76. Laco, M.N., et al., *Compromised mitochondrial complex II in models of Machado-Joseph disease.* Biochim Biophys Acta, 2012. **1822**(2): p. 139-49.
77. Durcan, T.M. and E.A. Fon, *Ataxin-3 and its e3 partners: implications for machado-joseph disease.* Front Neurol, 2013. **4**: p. 46.
78. Ran, F.A., et al., *Genome engineering using the CRISPR-Cas9 system.* Nat Protoc, 2013. **8**(11): p. 2281-2308.
79. Mandegar, M.A., et al., *CRISPR Interference Efficiently Induces Specific and Reversible Gene Silencing in Human iPSCs.* Cell Stem Cell, 2016. **18**(4): p. 541-53.
80. Jinek, M., et al., *A programmable dual-RNA-guided DNA endonuclease in adaptive bacterial immunity.* Science, 2012. **337**(6096): p. 816-21.
81. Ran, F.A., et al., *Double nicking by RNA-guided CRISPR Cas9 for enhanced genome editing specificity.* Cell, 2013. **154**(6): p. 1380-9.
82. Lalonde, S., et al., *Frameshift indels introduced by genome editing can lead to in-frame exon skipping.* PLoS One, 2017. **12**(6): p. e0178700.

83. Laflamme, C., et al., *Implementation of an antibody characterization procedure and application to the major ALS/FTD disease gene C9ORF72.* Elife, 2019. **8**.
84. Neves-Carvalho, A., et al., *Dominant negative effect of polyglutamine expansion perturbs normal function of ataxin-3 in neuronal cells.* Hum Mol Genet, 2015. **24**(1): p. 100-17.
85. Rodrigues, A.J., et al., *Absence of ataxin-3 leads to cytoskeletal disorganization and increased cell death.* Biochim Biophys Acta, 2010. **1803**(10): p. 1154-63.
86. Aguer, C., et al., *Galactose enhances oxidative metabolism and reveals mitochondrial dysfunction in human primary muscle cells.* PLoS One, 2011. **6**(12): p. e28536.
87. Soderholm, J.F., et al., *Importazole, a small molecule inhibitor of the transport receptor importin-beta.* ACS Chem Biol, 2011. **6**(7): p. 700-8.
88. Williams, J.A., et al., *New methods for monitoring mitochondrial biogenesis and mitophagy in vitro and in vivo.* Exp Biol Med (Maywood), 2017. **242**(8): p. 781-787.
89. Shi, Z., et al., *Ataxin-3 promotes testicular cancer cell proliferation by inhibiting anti-oncogene PTEN.* Biochem Biophys Res Commun, 2018. **503**(1): p. 391-396.
90. Bonanomi, M., et al., *The Toxic Effects of Pathogenic Ataxin-3 Variants in a Yeast Cellular Model.* PLoS One, 2015. **10**(6): p. e0129727.
91. Yan, W.Q., et al., *[Effect of nuclear receptor inhibitor importazole on the proliferation and apoptosis of multiple myeloma cells].* Zhonghua Xue Ye Xue Za Zhi, 2013. **34**(4): p. 323-6.
92. Chen, J. and Z.J. Chen, *Regulation of NF-kappaB by ubiquitination.* Curr Opin Immunol, 2013. **25**(1): p. 4-12.
93. Liu, T., et al., *NF-kappaB signaling in inflammation.* Signal Transduct Target Ther, 2017. **2**.
94. Wang, Q., C. Song, and C.C. Li, *Molecular perspectives on p97-VCP: progress in understanding its structure and diverse biological functions.* J Struct Biol, 2004. **146**(1-2): p. 44-57.
95. Muller-Rischart, A.K., et al., *The E3 ligase parkin maintains mitochondrial integrity by increasing linear ubiquitination of NEMO.* Mol Cell, 2013. **49**(5): p. 908-21.
96. Fiskin, E. and I. Dikic, *Parkin promotes cell survival via linear ubiquitination.* EMBO J, 2013. **32**(8): p. 1072-4.
97. Zhong, X. and R.N. Pittman, *Ataxin-3 binds VCP/p97 and regulates retrotranslocation of ERAD substrates.* Hum Mol Genet, 2006. **15**(16): p. 2409-20.
98. Doss-Pepe, E.W., et al., *Ataxin-3 interactions with rad23 and valosin-containing protein and its associations with ubiquitin chains and the proteasome are consistent with a role in ubiquitin-mediated proteolysis.* Mol Cell Biol, 2003. **23**(18): p. 6469-83.
99. Laco, M.N., et al., *Valosin-containing protein (VCP/p97) is an activator of wild-type ataxin-3.* PLoS One, 2012. **7**(9): p. e43563.
100. Wu, Y.L., et al., *Treatment with Caffeic Acid and Resveratrol Alleviates Oxidative Stress Induced Neurotoxicity in Cell and Drosophila Models of Spinocerebellar Ataxia Type3.* Sci Rep, 2017. **7**(1): p. 11641.
101. Goswami, A., et al., *Expression of expanded polyglutamine proteins suppresses the activation of transcription factor NFkappaB.* J Biol Chem, 2006. **281**(48): p. 37017-24.
102. Choubey, V., et al., *BECN1 is involved in the initiation of mitophagy: it facilitates PARK2 translocation to mitochondria.* Autophagy, 2014. **10**(6): p. 1105-19.

103. Pickford, F., et al., *The autophagy-related protein beclin 1 shows reduced expression in early Alzheimer disease and regulates amyloid beta accumulation in mice.* J Clin Invest, 2008. **118**(6): p. 2190-9.
104. Shibata, M., et al., *Regulation of intracellular accumulation of mutant Huntingtin by Beclin 1.* J Biol Chem, 2006. **281**(20): p. 14474-85.
105. Nascimento-Ferreira, I., et al., *Overexpression of the autophagic beclin-1 protein clears mutant ataxin-3 and alleviates Machado-Joseph disease.* Brain, 2011. **134**(Pt 5): p. 1400-15.
106. Friedman, J.R. and J. Nunnari, *Mitochondrial form and function.* Nature, 2014. **505**(7483): p. 335-43.
107. Dhillon, V.S. and M. Fenech, *Mutations that affect mitochondrial functions and their association with neurodegenerative diseases.* Mutat Res Rev Mutat Res, 2014. **759**: p. 1-13.
108. Livnat-Levanon, N. and M.H. Glickman, *Ubiquitin-proteasome system and mitochondria - reciprocity.* Biochim Biophys Acta, 2011. **1809**(2): p. 80-7.
109. Shanbhag, R., et al., *The emerging role of proteolysis in mitochondrial quality control and the etiology of Parkinson's disease.* Parkinsons Dis, 2012. **2012**: p. 382175.
110. Peng, J., et al., *A proteomics approach to understanding protein ubiquitination.* Nat Biotechnol, 2003. **21**(8): p. 921-6.
111. Nijhawan, D., et al., *Elimination of Mcl-1 is required for the initiation of apoptosis following ultraviolet irradiation.* Genes Dev, 2003. **17**(12): p. 1475-86.
112. Wang, H., et al., *Parkin ubiquitinates Drp1 for proteasome-dependent degradation: implication of dysregulated mitochondrial dynamics in Parkinson disease.* J Biol Chem, 2011. **286**(13): p. 11649-58.
113. Tanaka, A., et al., *Proteasome and p97 mediate mitophagy and degradation of mitofusins induced by Parkin.* J Cell Biol, 2010. **191**(7): p. 1367-80.
114. Dikic, I. and A. Bremm, *DUBs counteract parkin for efficient mitophagy.* EMBO J, 2014. **33**(21): p. 2442-3.
115. Durcan, T.M., et al., *USP8 regulates mitophagy by removing K6-linked ubiquitin conjugates from parkin.* EMBO J, 2014. **33**(21): p. 2473-91.
116. Cornelissen, T., et al., *The deubiquitinase USP15 antagonizes Parkin-mediated mitochondrial ubiquitination and mitophagy.* Hum Mol Genet, 2014. **23**(19): p. 5227-42.
117. Cunningham, C.N., et al., *USP30 and parkin homeostatically regulate atypical ubiquitin chains on mitochondria.* Nat Cell Biol, 2015. **17**(2): p. 160-9.
118. Ordureau, A., et al., *Quantitative proteomics reveal a feedforward mechanism for mitochondrial PARKIN translocation and ubiquitin chain synthesis.* Mol Cell, 2014. **56**(3): p. 360-75.
119. Wang, Y., et al., *Deubiquitinating enzymes regulate PARK2-mediated mitophagy.* Autophagy, 2015. **11**(4): p. 595-606.
120. Nakamura, N. and S. Hirose, *Regulation of mitochondrial morphology by USP30, a deubiquitinating enzyme present in the mitochondrial outer membrane.* Mol Biol Cell, 2008. **19**(5): p. 1903-11.
121. Akutsu, M., I. Dikic, and A. Bremm, *Ubiquitin chain diversity at a glance.* J Cell Sci, 2016. **129**(5): p. 875-80.

122. Yamano, K., N. Matsuda, and K. Tanaka, *The ubiquitin signal and autophagy: an orchestrated dance leading to mitochondrial degradation.* EMBO Rep, 2016. **17**(3): p. 300-16.
123. Matsumoto, M.L., et al., *K11-linked polyubiquitination in cell cycle control revealed by a K11 linkage-specific antibody.* Mol Cell, 2010. **39**(3): p. 477-84.
124. Morimoto, D. and M. Shirakawa, *The evolving world of ubiquitin: transformed polyubiquitin chains.* Biomol Concepts, 2016. **7**(3): p. 157-67.
125. Ou, Z., et al., *Autophagy Promoted the Degradation of Mutant ATXN3 in Neurally Differentiated Spinocerebellar Ataxia-3 Human Induced Pluripotent Stem Cells.* Biomed Res Int, 2016. **2016**: p. 6701793.
126. Hansen, S.K., et al., *Generation of spinocerebellar ataxia type 3 patient-derived induced pluripotent stem cell line SCA3.A11.* Stem Cell Res, 2016. **16**(3): p. 553-6.
127. Ouyang, S., et al., *CRISPR/Cas9-Targeted Deletion of Polyglutamine in Spinocerebellar Ataxia Type 3-Derived Induced Pluripotent Stem Cells.* Stem Cells Dev, 2018. **27**(11): p. 756-770.